

# Eclogite varieties and petrotectonic evolution of the northern Guatemala Suture Complex

Uwe Martens<sup>a,b</sup>, Tatsuki Tsujimori <sup>c</sup> and Juhn G. Liou<sup>b</sup>

<sup>a</sup>Tectonic Analysis Inc., Walnut Creek, CA, USA; <sup>b</sup>Department of Geological Sciences, Stanford University, Stanford, CA, USA; <sup>c</sup>Center for Northeast Asian Studies, Tohoku University, Sendai, Japan

## ABSTRACT

Field and petrologic characteristics of two new eclogite localities within the Guatemala Suture Complex (GSC) north of the Motagua Fault are presented. The Tuncaj Hill locality exposes a coherent body of retrogressed eclogite hundreds of metres long that is associated with serpentinite of the North Motagua Unit. The Tanilar River locality exposes numerous bands and lenses of eclogite hosted in sialic gneisses of the Chuacús Complex. The Tuncaj eclogite has a two-stage prograde evolution containing the peak assemblage Grt + Omp + Ttn + Czo + Zo ± Am, formed at temperatures <720°C. In contrast, eclogites of the Tanilar unit are characterized by the paragenesis Omp + Grt + Rt ± Phg ± Qtz ± Ep giving higher peak conditions of T = 720–830°C and P = 2.1–2.7 GPa, near the stability field of coesite. Previously obtained data and our thermobaric calculations suggest distinct petrotectonic evolutions for the various types of eclogites within the suture. The lawsonite eclogites south of the Motagua Fault were probably produced in a mature Farallon subduction zone during the Early Cretaceous. The northern high-pressure (HP) blocks in serpentinite mélange and coherent amphibolite bodies with eclogite relics were generated by the Early Cretaceous subduction of the proto-Caribbean lithosphere under the Great Caribbean Arc. A continental block, the North American passive margin, reached the arc's trench in the Campanian and was subducted to ca. 80 km depth, producing the eclogites of the Chuacús Complex. As the slab was delaminated and partially exhumed, the continental Chuacús became tectonically juxtaposed with HP blocks of the proto-Caribbean that had been accreted to the Caribbean plate forming the North Motagua Unit. The juxtaposed group migrated to mid-crustal level and was contemporaneously retrogressed under epidote-amphibolite facies conditions.

## ARTICLE HISTORY

Received 28 September 2016  
Accepted 4 October 2016

## KEYWORDS

Serpentinite- and gneissic-hosted eclogites; high-pressure metamorphism; Guatemala Suture Complex; Chuacús Complex eclogite; arc-continent collision

## 1. Introduction

Unravelling the complex evolution of the Caribbean–North America plate boundary requires understanding the fossil subduction and collision zones preserved in the various sutures that occur throughout this tectonic boundary (Figure 1(a)). Of these, the Guatemala Suture Complex (GSC) is particularly significant because it comprises not one, but several juxtaposed high-pressure (HP) metamorphic belts that record the subduction of both oceanic and continental lithospheres throughout the Cretaceous. The GSC includes two parallel but distinct serpentine-matrix eclogitic mélanges (South and North Motagua; e.g. Beccaluva *et al.* 1995; Harlow *et al.* 2004; Tsujimori *et al.* 2005, 2006a; Brueckner *et al.* 2009) separated by the Motagua Fault, an active left-lateral fault that constitutes the current boundary between the North American and

the Caribbean plates in Central America (e.g. Plafker 1976; Figure 1(b)). North of this fault, a third HP belt occurs, which is characterized by eclogites hosted in sialic gneisses of the Chuacús Complex (van den Boom 1972; Ortega-Gutiérrez *et al.* 2004; Ratschbacher *et al.* 2009; Martens *et al.* 2012).

The petrologic characteristics of the southernmost HP belt are well studied (e.g. Harlow *et al.* 2003; Tsujimori *et al.* 2005, 2006a). The belt includes eclogite, blueschist, and metasedimentary rocks characterized by lawsonite-bearing assemblages that record a very cold palaeogeotherm of ca. 5–7 km/°C near forbidden-zone *P–T* conditions (Tsujimori *et al.* 2006a, 2006b). In contrast, the mode of occurrence, microstructure, mineral chemistry, and *P–T* estimates of serpentinite- and gneiss-hosted eclogites north of the Motagua Fault have not been as thoroughly investigated. Furthermore, the tectonic processes responsible for

**CONTACT** Uwe Martens  [umartens@zoho.com](mailto:umartens@zoho.com)  Tectonic Analysis Inc., 1315 Alma Ave Ste 134, Walnut Creek, CA 94596, USA

Paper for *International Geology Review* Special Issue 'Subduction, fluids, and accessory minerals: A celebration of the career of Sorena S. Sorensen' Editors Barb Dutrow, Jinny Sisson, Sarah Penniston-Dorland, and W.G. Ernst

 Supplemental data for this article can be accessed [here](#).

© 2016 Informa UK Limited, trading as Taylor & Francis Group

juxtaposing the distinct HP belts remain enigmatic (e.g. Pindell *et al.* 2011).

We present a detailed investigation of gneiss-hosted continental eclogites and mappable oceanic amphibolites with eclogite relics in the Sierra de Chuacús of Central Guatemala, north of the Motagua Fault (Figure 1). We describe their field characteristics, parageneses, mineral compositions, and  $P$ - $T$  estimates of metamorphism. Based on these data and available geochronologic data, we propose a model that accounts for the juxtaposition of gneiss-hosted eclogites with serpentinite mélangé and mappable bodies of eclogite retrogressed to amphibolite in the Sierra de Chuacús, north of the Motagua Fault.

## 2. Regional setting

The current left-lateral displacement between the North America and Caribbean plates in Central America (Figure 1(a)) is accommodated by a series of E–W-trending faults located in the region between the Polochic Valley in Guatemala and the Jocotán Valley in Honduras (e.g. Schwartz *et al.* 1979; Guzmán-Speziale *et al.* 1989; Figure 1(b)). These faults and shear zones were produced by the oblique Late Cretaceous collision of the Great Caribbean Arc with the passive margin of North America, and the subsequent left-lateral migration of terranes (e.g. the Chortis Block) from Mexico's Pacific

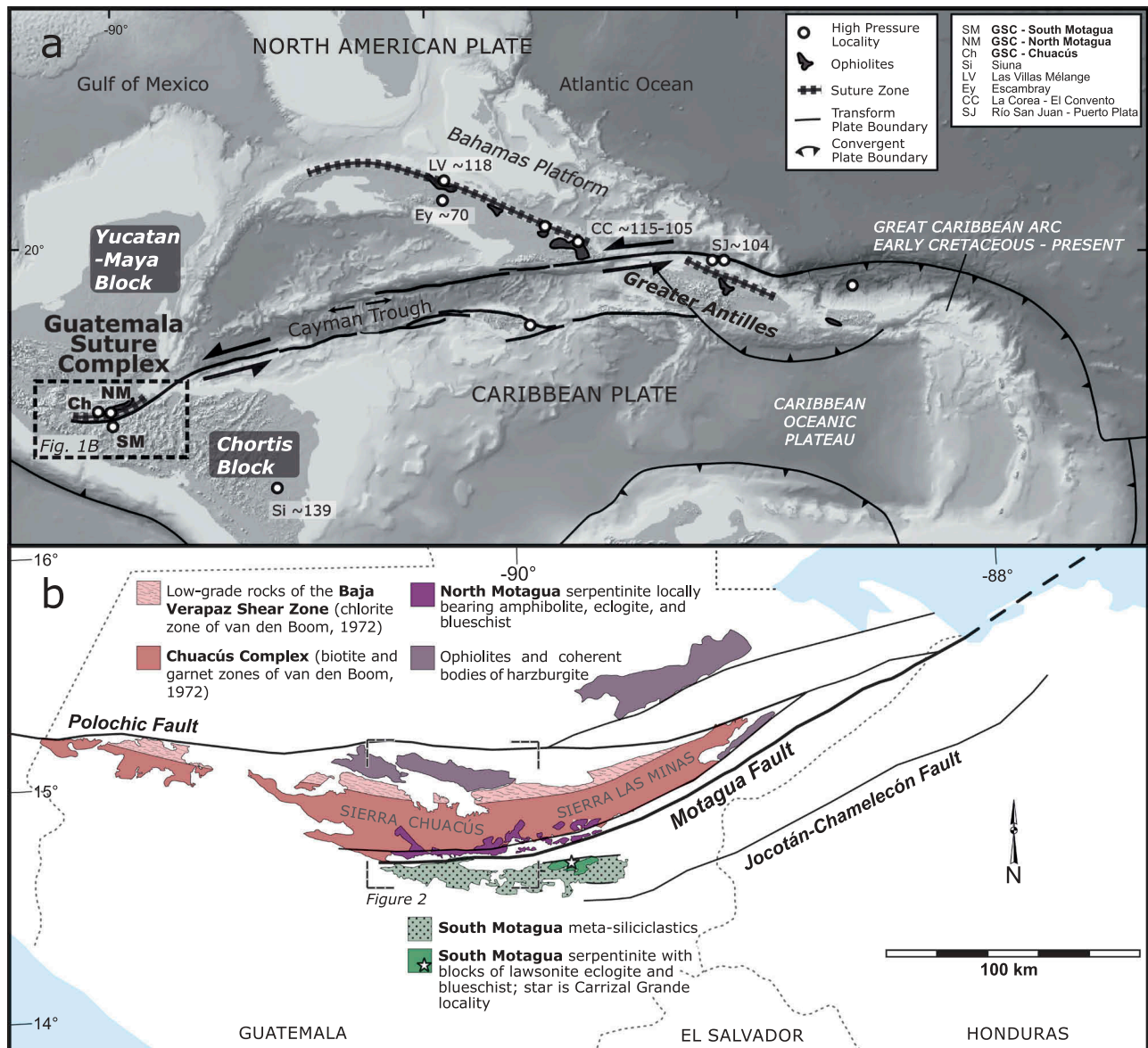


**Figure 1.** (a) Tectonic outline of the North America–Caribbean plate boundary showing the location of the main suture zones, ophiolites, and HP localities. Numbers adjacent to HP locality abbreviations are the age of the HP event in Ma (Baumgartner *et al.* 2008; Krebs *et al.* 2008; Stanek *et al.* 2009; Blanco-Quintero *et al.* 2011). (b) Simplified geologic map of Central Guatemala and Northern Honduras showing the main metamorphic units comprising the Guatemala Suture Complex and the main faults at the plate boundary. Modified from Bonis *et al.* (1970).

to their current position in Central America (e.g. Pindell *et al.* 1988; Keppie and Morán-Zenteno 2005). The collision and the displacement of the Chortis Block produced a complex array of fault-bounded, E–W-trending tectonic slivers containing serpentinite, serpentinite mélangé, amphibolite, metasedimentary mélangé, ophiolites, possibly pieces of island arcs, mantle harzburgite, and sialic gneisses that host eclogites (see reviews by Donnelly *et al.* 1990; Martens *et al.* 2007). We refer to this array of geologic units as the GSC although the names Motagua Suture Zone and Guatemala Suture Zone have also been used (e.g. Bertrand and Vuagnat 1975; Beccaluva *et al.* 1995; Brueckner *et al.* 2009; Ratschbacher *et al.* 2009). Three main units that contain HP rocks have been recognized in the suture complex (Figure 1(b)): the South Motagua emplaced onto the continental basement of the Caribbean Plate (Chortis Block), the North Motagua emplaced onto the continental basement of the North American Plate (Maya Block), and the Chuacús Complex (van den Boom *et al.* 1971; Ortega-Gutiérrez *et al.* 2004), which is the continental basement of the Maya Block (Dengo 1969) and represents the southernmost part of the North American Plate (Donnelly *et al.* 1990). A minority of authors have questioned the autochthony of the Chuacús Complex and they consider it a continental suspect terrane (e.g. Ortega-Gutiérrez *et al.* 2007).

### 2.1. South Motagua Unit

The South Motagua Unit (Figure 1(b)) includes serpentinite, serpentinite mélangé, low-grade metasediments, metasedimentary mélangé, mylonitized gabbro and diorite, low-grade pillow lava, greenstone, chert, blueschist, jadeitite, amphibolite, and eclogite (Bertrand and Vuagnat 1975, 1976, 1977, 1980; Beccaluva *et al.* 1995; Giunta *et al.* 2002; Harlow *et al.* 2003). A key locality is Carrizal Grande (Figure 1(b)), ca.12 km south of the Motagua Fault, where a large number of loose blocks (<10 m) of lawsonite eclogite and other HP rocks are exposed in the gorge of creeks (Tsujiomor *et al.* 2005, 2006a). Some eclogite blocks contain bands of Grt + Qtz + Mca schist (mineral abbreviations from Siivola and Schmidt 2007), suggesting that the protolith was a mixture of mafic rocks and semipelagic sediments. Serpentinite associated with eclogitic blocks is composed of schistose, friable antigorite.

The petrologic and microstructural features of lawsonite eclogites indicate three stages of metamorphism. The prograde stage is characterized by Grt + Omp/Jd + Lws + Chl + Rt + Qtz ± Phg, recording an eclogite-facies path from  $T \approx 300^\circ\text{C}$  and  $P > 1.1$  GPa to  $T \approx 480^\circ\text{C}$  and  $P \approx 2.6$  GPa (Table 1). Such conditions reflect a very low

**Table 1.** Comparison of key features of the main HP units that compose the Guatemala Suture Complex.

| Key Reference                             | Lawsonite eclogite, South Motagua Unit |                            | Epidote eclogite, North Motagua Unit  |                            | Coherent amphibolite with eclogite relics, North Motagua Unit  |  | Eclogite lenses and bands in Chuacús Complex                 |                                   | HP Rocks in the BVSZ  |                            |  |
|---|--|----------------------------|---|----------------------------|--|--|--|-----------------------------------|---|----------------------------|--|
|   | Tsujiomor <i>et al.</i> (2006a,2006b)  | Oceanic Antigorite schist  | Minor chert and Grt + Qtz + Wmca schist<br>Grt + Omp/Jd + Lws + Chl + Rt + Qtz ± Phg<br>$T \approx 480^\circ\text{C}$ and $P \approx 2.6$ GPa | Oceanic Antigorite schist  | Chert as blocks in mélangé.<br>Grt + Omp + Zo + Phg + Pg + Rt + Qtz<br>$T \approx 600\text{--}650^\circ\text{C}$ and $P \approx 2.0\text{--}2.3$ GPa | Oceanic Mappable amphibolites mostly contained in serpentinites<br>Not Present | Grt + Omp + Ttn + Czo + Zo ± Amph<br>$T < 720^\circ\text{C}$ | Oceanic Quartzofeldspathic gneiss | Abundant psammitic, semi-pelitic, and pelitic. The latter with Qtz + Wmca + Cld ± Ky ± Chl ± St<br>Omp + Grt + Rt ± Phg ± Qtz ± Ep<br>Up to $\sim 2.7$ GPa and $\sim 720\text{--}800^\circ\text{C}$ | Continental<br>Not present | Abundant psammitic, semi-pelitic, and pelitic. Low grade. Semipelitic rocks with Chl + Phg (3.4 Si pfu)<br>1 GPa and $300^\circ\text{C}$<br>(Sub) greenschist facies |
| Metasediment association                  |  |                            |   |                            |  |  |  |                                   |   |                            |  |
| Peak assemblage of metamorphic protoliths |  |                            |   |                            |  |  |  |                                   |   |                            |  |
| Peak P and T                              |  |                            |   |                            |  |  |  |                                   |   |                            |  |
| Metamorphic facies of retrogression       |  |                            |   |                            |  |  |  |                                   |   |                            |  |
| Age of protolith                          | Unknown. Perhaps Triassic-Jurassic.    | Unknown. Perhaps Jurassic. | Unknown. Perhaps Jurassic.  | Unknown. Perhaps Jurassic. | Unknown. Perhaps Jurassic.   | Unknown. Perhaps Jurassic.   | Precambrian, Ordovician, Triassic, Jurassic.                 |                                   |   |                            |  |
| Age of jadeitite                          | $\sim 154$ Ma                          | $\sim 154$ Ma              | $\sim 95$ Ma  | $\sim 95$ Ma               | Not present  | Not present  | Not present  |                                   |   |                            |  |
| Age of Peak HP                            | 150–125 Ma                             | 137–118 Ma                 | $\sim 75\text{--}65$ Ma   | $\sim 75\text{--}65$ Ma    | Not dated  | $\sim 76$ Ma   | $\sim 76$ Ma   |                                   |   |                            |  |
| Time Onset of Cooling                     | $\sim 120$ Ma                          | $\sim 120$ Ma              | $\sim 75\text{--}65$ Ma   | $\sim 75\text{--}65$ Ma    | Possibly $\sim 75\text{--}65$ Ma   | $\sim 75\text{--}62$ Ma  | $\sim 75\text{--}62$ Ma                                      |                                   |   |                            | unconstrained  |

geotherm of ca. 5°C/km. Early retrogression conditions of  $T \approx 400^\circ\text{C}$ ,  $P \approx 1.8$  GPa formed an eclogite assemblage including Grt + Omp + Phg. Finally, a late blueschist-facies overprint is characterized by the assemblage Gln + Lws + Chl + Ttn + Qtz  $\pm$  Phg (Tsuji-mori *et al.* 2005, 2006a).

## 2.2. North Motagua Unit

The North Motagua Unit occurs north of the Motagua Fault (e.g. Giunta *et al.* 2002; Figure 1(b)) and is characterized by antigorite schist with minor metre-scale blocks of garnet amphibolite with relict omphacite, jadeitite, omphacite-taramite rock, omphacite, epidote eclogite, and blueschist (Harlow 1994). Associated with these are garnet amphibolite bodies that are coherent and sufficiently large to be mapped at 1:125,000 scale (van den Boom *et al.* 1971; Bonis 1993; Figure 2). One such body is exposed at Tuncaj Hill, a hitherto undescribed locality where eclogite relics in amphibolite are well preserved.

One metre-scale block of serpentinite-hosted eclogite north of the Motagua Fault contains the peak assemblage Grt + Omp ( $\text{Jd}_{30-51}\text{Aug}_{48-65}\text{Aeg}_{<6}$ ) + Zo + Phg (3.5 Si apfu) + Pg + Rt + Qtz (Tsuji-mori *et al.* 2004). Garnet porphyroblasts display two discontinuous growth zones; the garnet cores ( $\text{Alm}_{46-52}\text{Gr}_{525-31}\text{Prp}_{18-26}\text{Sps}_{<4}$ ) contain inclusions of Omp + Rt, whereas the garnet

rims are less magnesian ( $\text{Alm}_{45-53}\text{Gr}_{527-31}\text{Prp}_{14-20}\text{Sps}_{<4}$ ) and contain inclusions of Hbl + Ttn. Thermobarometric calculations indicate that northern Motagua eclogites equilibrated at  $T \approx 600-650^\circ\text{C}$  and  $P \approx 2.0-2.3$  GPa (Tsuji-mori *et al.* 2004; Table 1), recording a higher geothermal gradient when compared with eclogites south of the fault. A retrogression assemblage including amphibole and albite partially replaced eclogite-facies assemblages.

## 2.3. The Chuacús Complex

Ortega-Gutiérrez *et al.* (2004) recognized that eclogites of the GSC not only are hosted in serpentinites as described above, but also occur as bands and lenses variably retrogressed to amphibolite enclosed in high-grade quartzofeldspathic gneisses of the Chuacús Complex (Figures 1 and 2).

The Chuacús Complex is an E-W-elongated metamorphic belt north of the Motagua Fault characterized by Chl-bearing assemblages in the north and by Bt  $\pm$  Grt-bearing assemblages in the south (Figure 1(b); van den Boom 1972). The highlands of the Sierra de Chuacús are dominated by ortho- and paragneisses containing Qtz + Ab/Olig + Wmca  $\pm$  Ep/Zo  $\pm$  Grt  $\pm$  Bt  $\pm$  Ttn  $\pm$  Rt  $\pm$  Am  $\pm$  Chl  $\pm$  Omp  $\pm$  Cld  $\pm$  Cal  $\pm$  Aln. Other rock types include amphibolites with relict eclogite-facies minerals, pelitic

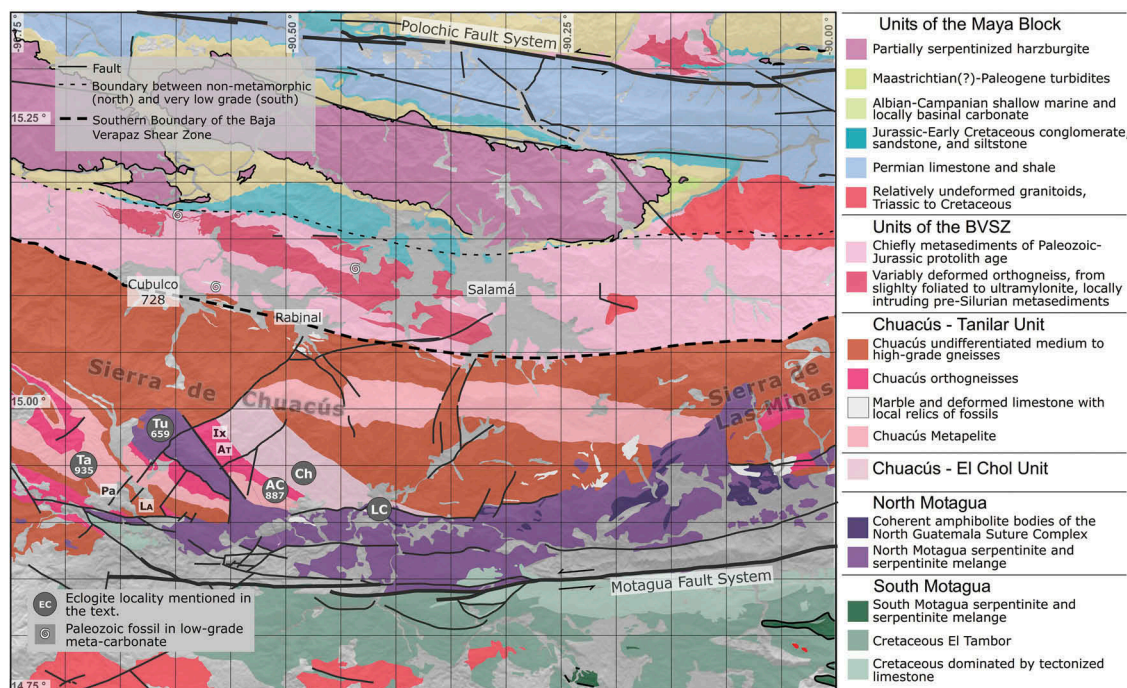


**Figure 2.** Generalized geologic map of Central Guatemala showing units of the Maya Block passive margin stratigraphy, the Baja Verapaz Shear Zone (BVSZ), the Chuacús Complex, and the North and the South Motagua units. Grey circles are eclogite localities; AC, Agua Caliente; Ch, El Chol; LC, La Canoa; Ta, Tanilar; Tu, Tuncaj. Other abbreviated localities are AT, Agua Tibia; Ix, Ixchel; LA, Los Altos; Pa, Pachalum. Numbers are samples mentioned in the text. Modified from Martens (2009), and references therein.

gneisses bearing  $Ky + Cld \pm St$ , and calcsilicates bearing  $Trm + Ttn + Wmca + Ol$  (van den Boom 1972; Ortega-Gutiérrez *et al.* 2004). The predominant assemblages suggest epidote-amphibolite facies conditions of  $P \approx 0.65\text{--}0.8$  GPa and  $T \approx 450\text{--}600^\circ\text{C}$ , but the mineral chemistry of relict eclogite-facies assemblages in mafic protoliths indicates near ultra-high pressure conditions of  $P \approx 2.0\text{--}2.4$  GPa and  $T \approx 600\text{--}750^\circ\text{C}$  (Ratschbacher *et al.* 2009; Martens *et al.* 2012; Table 1).

A further useful subdivision of the Chuacús Complex is based on the complexity of the ductile structures. The rocks characterized by a single dominant foliation and simple folding constitute the Tanilar unit, which is best exposed along the gorges of the Tanilar and Agua Caliente rivers (Figure 2 and Figure 3(a)). The Tanilar unit is chiefly composed of orthogneisses, metapelites, two-mica gneisses, marble, and metamafic bands and boudins. Rocks characterized by complexly refolded leucocratic and melanocratic bands constitute the El

Chol unit, which is composed of banded amphibolites with eclogite relics and various generations of metagranites, such as variably deformed pegmatites and leucosomes (Figure 3(b)).

#### 2.4. The Baja Verapaz Shear Zone (BVSZ) and its significance

Ortega-Obregón (2005) defined a kilometre-scale shear zone in the Rabinal–Salamá area, whose extent coincides with the chlorite zone of the Chuacús Complex defined by van den Boom (1972; Figure 2). In our view, both authors are correct as the recognized area is both a zone characterized by chlorite and a region of deformation under greenschist-facies conditions involving various igneous and sedimentary protoliths. The same unit is named the Achí terrane by Ortega-Gutiérrez *et al.* (2007) and the Rabinal complex by Ratschbacher *et al.* (2009). Deformation was very heterogeneous, ranging from relatively undeformed outcrops, where pre-deformation contacts are preserved, to zones of mylonite and ultramylonite.

In subsequent articles, the BVSZ was reinterpreted to be a discrete reverse fault instead of a shear zone up to 12 km wide. Furthermore, the discrete fault was proposed to be a major terrane boundary (Ortega-Gutiérrez *et al.* 2007; Ortega-Obregón *et al.* 2008). Our field observations are consistent with the original definition of the BVSZ, but we could not find the proposed discrete, brittle fault of regional extent. Indeed, the kilometre-wide shear zone juxtaposes nearly-unmetamorphosed rocks on its northern fringe with amphibolite-facies rocks some 10 km on the south (Figure 2; Ortega-Obregón 2005). We interpret the zone as juxtaposing disparate structural levels of North American crust and not as a far-travelled tectonostratigraphic terrane.

The eclogites are restricted to the southern portion of the Chuacús and progressively lower-grade rocks occur towards the north, culminating in the chlorite zone at the northern boundary. Evidence for relatively high  $P$  is present at all metamorphic grades. In the south the gneisses bear eclogite; further north pelitic schist contains  $Grt + Cld$  devoid of  $Bt$ ; in the chlorite zone (or the BVSZ) white mica is phengite with  $Si = 3.3\text{--}3.4$  apfu (Solari *et al.* 2013; Table 1).

### 3. Available geochronology of the HP metamorphic events

There is a sharp contrast in the age of eclogites among the various HP belts recognized in the GSC (Table 1). Sm–Nd mineral isochrons from South Motagua eclogites yielded ages of  $131.7 \pm 1.7$  and  $132.0 \pm 4.6$  Ma, which



**Figure 3.** Field photographs showing the main outcrop-scale structural features of the Chuacús Complex. (a) Banded gneiss of the Tanilar unit showing one dominant foliation. (b) Complexly folded banded polymetamorphic gneisses of the El Chol Unit.

are analogous to the  $130.7 \pm 6.3$  Ma isochron from serpentinite-hosted eclogite sampled north of the fault (Brueckner *et al.* 2009). Given their Early Cretaceous age, these older eclogites must have been produced by the subduction of either Farallon or proto-Caribbean oceanic lithosphere (e.g. Pindell *et al.* 1988). In contrast, eclogites of the Chuacús Complex have yielded a  $77 \pm 13$  Ma Sm–Nd mineral isochron and a  $75.5 \pm 1.9$  Ma U–Pb age obtained in zircon rims formed during the eclogite stage (Martens *et al.* 2012). These ages are interpreted to be the product of a Late Cretaceous collision of the Great Caribbean Arc with the southernmost passive margin of North America (e.g. Pindell and Barrett 1990).

The ages of formation of serpentinite-hosted jadeitites in the North and South Motagua units are also different. A sample of phengite jadeitite from the south has yielded large zircons and a very well-constrained concordia age of  $153.7 \pm 3.5$  Ma (MSWD = 2; Fu *et al.* 2009). Jadeitite zircons from the northern serpentinite mélange are younger, yielding a mean age of  $94 \pm 4$  Ma (MSWD = 6.7; Yui *et al.* 2010). The contrast in ages was further confirmed by *in situ* dating of jadeitite zircon in thin sections (Flores *et al.* 2013).

The timing of the retrograde event and the onset of cooling are also distinct.  $^{40}\text{Ar}/^{39}\text{Ar}$  white mica (phengite) ages from HP rocks from the southern belt are in the range 125–113 Ma (most cluster at ca. 120 Ma); these Early Cretaceous ages have been interpreted as the time of fluid infiltration during blueschist-facies retrogression of South Motagua eclogites.  $^{40}\text{Ar}/^{39}\text{Ar}$  white mica ages of eclogite from the northern serpentinite mélange are in the range 77–65 Ma, which have been interpreted as the onset of cooling after amphibolite-facies overprint (Harlow *et al.* 2004). Interestingly, these Late Cretaceous ages are analogous to the timing of amphibolite-facies overprint of the Chuacús Complex and onset of its cooling. Metamorphic zircon rims possibly produced during the overprint stage have yielded 75–70 Ma, whereas most cooling ages obtained by Rb–Sr, K–Ar, and  $^{40}\text{Ar}/^{39}\text{Ar}$  dating of white mica and amphibole are in the range of 76–62 Ma (Sutter 1979; Ortega-Gutiérrez *et al.* 2004; Ratschbacher *et al.* 2009). The above age-correlation and the latest Cretaceous intrusion of pegmatite dikes into both the Chuacús Complex and North Motagua serpentinites strongly suggest that these HP units had been juxtaposed by the Late Cretaceous (Ratschbacher *et al.* 2009; Martens *et al.* 2012).

#### 4. Field characteristics of eclogites in the Sierra de Chuacús, north of the Motagua Fault

As noted above, field transects across the Sierra de Chuacús showed that most gneiss-hosted eclogites and

amphibolites with eclogite relics occur in the southern flank and central highlands of the Sierra de Chuacús (individual localities shown in Figure 2). Gneiss-hosted Grt + Ep amphibolites do occur in the northernmost part of the mountain range; however, none of the studied thin sections contains relics of omphacite. Further north, low-grade meta-granites in the BVSZ area contain phengite with high-celadonite component (Solari *et al.* 2013). Such a progressive decrease in metamorphic grade suggests southward subduction polarity with a high  $P$ – $T$  gradient for subduction-zone metamorphism of the Chuacús Complex.

Furthermore, previously mapped coherent amphibolite bodies of the North Motagua Unit in the Sierra de Chuacús contain domains of a prior eclogite-facies assemblage (e.g. La Canoa and Tuncaj localities; Figure 2). We surmise that the bulk of these coherent bodies were once eclogites produced from blocks of subducted oceanic crust.

Reconnaissance fieldwork in the Sierra de Las Minas confirmed the presence of eclogites associated with serpentinite of the North Motagua Unit. However, no eclogites or eclogitic relics were found in amphibolites enclosed within high-grade sillimanite-bearing sialic gneisses. We speculate that high-grade granitic gneisses in this region may have a different Late Cretaceous geologic history or that intense retrogression during exhumation may have completely erased relict eclogite-facies assemblages. We prefer the latter suggestion as abundant migmatites and sillimanite-bearing assemblages are common in the area.

#### 4.1. Eclogites in the Tanilar unit of the Chuacús Complex

The Tanilar River section (Figure 2) exposes hitherto undescribed eclogite and Ep + Omp pods and bands 1–30 cm thick (Figure 4(a–b)) at the margin of lineated orthogneiss. Towards the south, the river gorge exposes lenses of both Bt + Grt gneisses and mafic schist containing Ep + Omp; the exposed section ends with quartzite and Grt + Wmca schist bearing minor kyanite. The metapelites lack interfoliated mafic bands and are cut by massive pegmatites.

Amphibolitized eclogites also occur as decimetre-scale boudins and bands 20–150 cm thick at the Agua Caliente River section (Figure 4(c)); these rocks are concordant with hosted orthogneisses and semi-pelitic and psammitic paragneiss that exhibit one dominant foliation dipping W–SW. The retrogressed eclogite bodies are interpreted as metamorphosed mafic dikes or concordant sills or flows associated with the sedimentary protolith. These mafic pods are variably boudinaged and disrupted by ductile deformation; some mafic

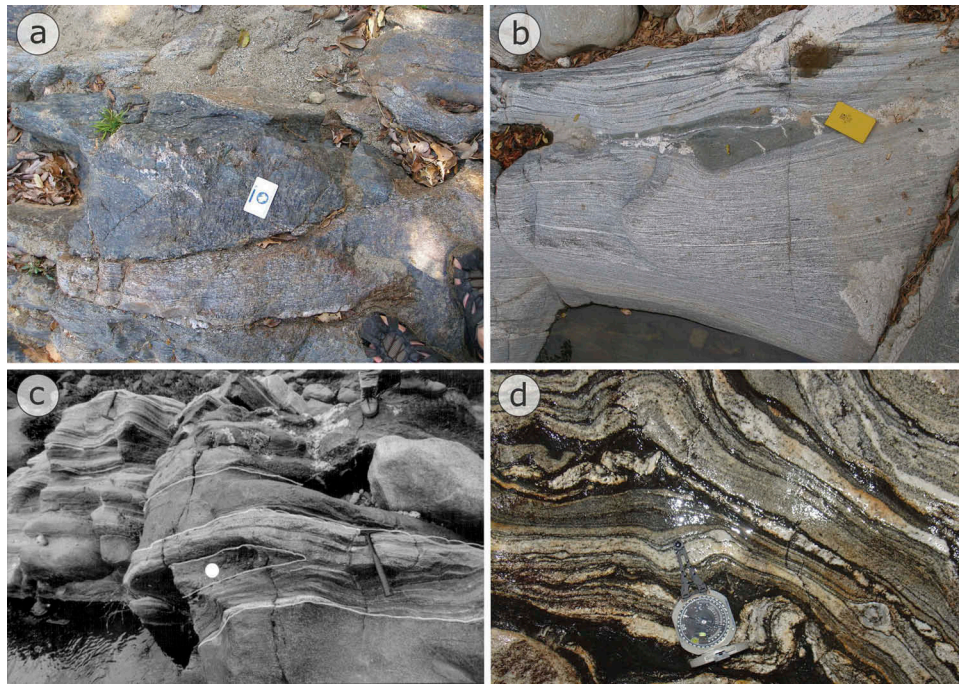


**Figure 4.** Field photographs of eclogite occurrence in the northern Guatemala Suture Complex. (a) Eclogite as lens (centre) and as band (bottom) hosted in Triassic orthogneiss at Agua Caliente and (b) boudinaged omphacite + epidote rock with pegmatite in boudin neck contained in orthogneiss at Tanilar. (c) Lens of eclogite in the core of isoclinal fold (white dot) in gneisses at Agua Caliente. (d) Amphibolite with eclogitic relics in the convolute banded gneisses at El Chol.

bands occur in the core of isoclinal folds. Most Agua Caliente eclogites are fine-grained, black in outcrop, and variably overprinted by amphibolite assemblages that contain coarse-grained centimetre-scale amphibole and plagioclase crystals. Eclogites also occur as centimetre-scale, irregular domains in amphibolites enclosed by banded gneiss. Orthogneisses at Agua Caliente have calc-alkaline geochemistry and were possibly produced in an arc setting (Solari *et al.* 2011). Some intrusive contacts are preserved despite deformation, and U–Pb zircon geochronology has demonstrated Triassic protolith ages (Ratschbacher *et al.* 2009; Martens *et al.* 2012).

At Los Altos (Figure 2), decimetre-scale bands of omphacite-bearing rocks occur interbedded in semi-pelitic paragneiss. The rock contains an assemblage including Qtz + Omp + Grt + Zo + Ttn and may have a sedimentary, calc-silicate protolith. The rare Ep + Omp pods up to 1 m in length hosted in gneiss and also occur 500 m upstream from the bridge over the Agua Tibia River, and another is present along the Agua Tibia–Ixchel road (Figure 2). These pods are composed of Omp + Ep + Ap and are overprinted by poikiloblastic Am + Ab.

#### 4.2. Eclogites in the El Chol unit

The El Chol unit is well exposed along the rivers and creeks around the town of El Chol (Figure 2). In contrast to other

Chuacús gneisses and eclogites, the structural features at El Chol are very complex (Figures 3 and 4(d)), including various generations of leucocratic and mafic bands with low-angle cross-cutting relations, various generations of folds, mylonitic bands with relict porphyroclasts, and eclogite relics. Previous geochronology has yielded components with Palaeozoic to Triassic ages (Solari *et al.* 2011). Most mafic bands at El Chol are fine-grained garnet amphibolite. Although almost black in outcrop, these rocks contain relics of omphacite and rutile. Furthermore, rare centimetre-scale relict eclogite-facies domains are preserved. These domains do not seem structurally controlled, but are probably the product of low permeability, limiting retrogression fluid flow and reactions.

#### 4.3. Eclogites in coherent amphibolite bodies

In the Sierra de Chuacús, coherent bodies of amphibolite tens to hundreds of metres in size (Figure 2) also contain centimetre- to decimetre-scale domains of relict eclogite minerals. Some of these bodies are large enough to be mapped at the 1:125,000 scale (van den Boom *et al.* 1971; Bonis 1993); most mafic bodies occur near serpentinite, but some are also associated with quartzofeldspathic gneiss, possibly separated by faults. Two examples are the amphibolite bodies with eclogite relics at La Canoa and at Tuncaj Hill (Figure 2). On the

banks of the Motagua River in La Canoa, an amphibolite body several hundred metres long is faulted against antigorite schist of the North Motagua Unit, and against marble and gneiss of the Chuacús Complex. The exposure at Tuncaj is strongly weathered, but amphibolite saprolite can be traced for >100 m along dirt roads. Irregular domains of eclogite are preserved within the large amphibolite body. Overall, amphibolite and eclogite at Tuncaj are associated with a large serpentinite unit, but the actual contact is covered (Figure 2).

## 5. Analytical procedures

Mineral chemistry was determined with a focused beam (<2 µm) using the JEOL 733A electron microprobe at Stanford University operated at 15 nA beam current and 15 kV accelerating voltage, and calibrated on natural mineral standards. Raw counts of Si, Al, Fe, Mg, Mn, K, Na, Ca, Cr, and Ti were collected for 20 s and converted to wt.% by the CITZAF correction procedure.

Garnet was recalculated in terms of Alm, Prp, Grs, and Sps components. Cpx analyses were recalculated in terms of (Di + Hd), Jd, Aeg, Ca-Tschermak, and Opx molecules; the latter two components were very low and analyses were further recalculated to (Di + Hd) + Jd + Aeg = 100% and classified based on Morimoto (1988). Amphiboles were classified according to Leake *et al.* (1997) and Leake *et al.* (2004).

Thermobarometry of eclogites was calculated using the spreadsheet of Krogh Ravna and Terry (2004). To obtain the highest pressure attained at the eclogite facies, Grt composition with maximum  $(X_{\text{Grs}})^2 \times X_{\text{Prp}}$ , Cpx composition with maximum  $X_{\text{Jd}}$ , and Phg with maximum  $X_{\text{Cel}}$  were used (Carswell *et al.* 2000). The spreadsheet uses the Phg solid solution model of Holland and Powell (1998), the Grt activity model of Ganguly *et al.* (1996), and the Cpx activity model of Holland (1990).

Thermobarometry of eclogites is critically dependent on the relation between  $T$ ,  $P$ , and composition for the  $\text{Fe}^{2+}$ -Mg exchange between Grt and Cpx, which is well constrained by multiple regression (e.g. Ravna 2000). However, this thermometer is very sensitive to uncertainty in the estimation of  $\text{Fe}^{3+}$  in Cpx, especially in Omp or in Fe-poor Cpx (Ravna 2000; Proyer *et al.* 2004). In the absence of Mössbauer analyses,  $\text{Fe}^{3+}$  is estimated using stoichiometry and charge balance effectively recalculating to four cations (Hamm and Vieten 1971; Droop 1987) or allocating  $\text{Fe}^{3+}$  only for alkalis in excess of Al (or  $\text{Fe}^{3+} = \text{Na} - \text{VIAl} - \text{Cr} - 2\text{Ti}$ ), effectively assuming  $\text{IVAl} = 0$  (Cawthorn and Collerson 1974; Lindsley 1983, and references therein).

Although neither method is completely satisfactory, in cases where  $X_{\text{Jd}} > 20$  mol%, the calculation based on excess Na over Al seems more reliable (Cawthorn and Collerson 1974; Carswell *et al.* 1997). We have therefore preferred it in our  $P$  and  $T$  estimations. The charge balance approach seems to overestimate  $\text{Fe}^{3+}$ , producing an artificially high distribution coefficient, which translates into underestimating the temperature (Ravna 2000; Krogh Ravna and Terry 2004). Uncertainty of such temperature estimates (disregarding potential exchange during retrogression) ranges from  $\pm 30^\circ\text{C}$  (Krogh Ravna and Terry 2004) up to  $\pm 250^\circ\text{C}$  (Proyer *et al.* 2004).

## 6. Petrography and mineral chemistry

We characterized Chuacús eclogites and amphibolites bearing relict HP phases from the Tanilar unit at the type locality (samples of the 935 series; localities shown in Figure 2) and the Agua Caliente River (887 series). These were compared with an amphibolite at the northern fringe of the Sierra de Chuacús at Cubulco (sample 728). A representative sample of relict eclogite in coherent bodies of amphibolite of the North Motagua Unit was collected at Tuncaj, near the highest ridge of the mountain range (series 659). The mineral parageneses and key petrographic and compositional features are summarized in Tables 2–3. A more detailed description of the petrography and the mineral chemistry can be found in the supplementary materials.

### 6.1. Gneiss-hosted eclogites at the Tanilar river section

Sample 935 K is a cobble collected from the bed of the Tanilar River. The rock is a Grt + Omp + Rt + Ep eclogite partially retrogressed to an assemblage of poikiloblastic Am + Pl (Table 2). Accessory phases include Zrn and Ap. The eclogite-facies assemblage is granuloblastic and grain size is ca. 0.3 mm (Figure 5). Zircons of this rock occur in the matrix and as inclusions in garnet and pyroxene, and they have been dated by U–Pb, yielding an age of 76 Ma for the HP event (Martens *et al.* 2012). In eclogite domains, garnet is idioblastic and has a relatively homogeneous composition (Figure 6) of  $\text{Alm}_{56}\text{Prp}_{17}\text{Grs}_{26}\text{Sps}_{<2}$  and  $\text{Fe}\#$  is  $0.77 \pm 0.02$  (Supplementary Table 1), whereas the outermost 25–75 µm rim contains slightly higher Alm and lower Grs. Omphacite of the sample has compositions of  $\text{Di}/\text{Hd}_{56-62}\text{Jd}_{30-35}\text{Aeg}_{7-11}$  (Supplementary Table 2).

Sample 935 L, also from the Tanilar River, is a granuloblastic eclogite cobble that was partly retrogressed to an assemblage of Am + Pl. The rock is similar to eclogite

**Table 2.** Mineral parageneses of eclogite sample series 935 from Tanilar during prograde, peak, and retrogression stages of metamorphism, including key petrographic features and mineral compositions.

| Tanilar River cobble, sample 935 K |            |   |   | Tanilar River, sample 935 RI |  |  |  |
|------------------------------------|------------|---|---|------------------------------|--|--|--|
|                                    | Prog       | Peak  | Retro   |                              | Prog   | Peak   | Retro  |
| Grt                                |            | Alm <sub>54</sub> Prp <sub>11</sub> GrS <sub>26</sub> Sp <sub>2</sub><br>Inclusions of Zrn,<br>Ttn, Am            | outer rim Alm <sup>+</sup> , Grs-<br>Partially resorbed | Am                           |  | ?  | poikiloblastic<br>magnesirotaramite  |
| Cpx                                |            | Omp<br>~Di/Hd <sub>60</sub> Jd <sub>33</sub> Aeg <sub>7</sub>   | Resorbed +<br>symplectite; sodic Di                     | Grt                          | ?  | Alm <sub>54</sub> Prp <sub>11</sub> GrS <sub>34</sub> Sps <sub>1</sub>           | Partially resorbed<br>Alm <sub>55</sub> Prp <sub>13</sub> GrS <sub>28</sub> Sps <sub>1</sub> |
| Rt                                 |            |   |   | CPX                          |  | Poorly preserved<br>Omp  | Symplectite  |
| Ep/Zo                              |            |   |   | Rt                           |  | Matrix and inclusion<br>in Grt,  |  |
| Zrn                                |            | HP metamorphic<br>rims – 76 Ma old  |   | Qtz                          |  |  |  |
| Am                                 | Blue       |   | Poikiloblastic  | Pl                           | .....?   |  | Ab <sub>90</sub>   |
| Pl                                 | .....?     |   | Poikiloblastic  | Czo                          |  |  |  |
| Ttn                                |            |   | Some with Rt cores                                      | Cb                           |  |  |  |
|                                    |            |   |   | Ttn                          |  |  | Rt cores   |
|                                    |            |   |   | Wmca                         |  | 3.37 Si apfu (cores)   | Lower Cel component<br>(outer part of crystals)  |
|                                    |            |   |   | Bt                           |  |  | From Phg   |
| Tanilar River cobble, sample 935 L |            |   |   | Tanilar River, sample 935 S  |  |  |  |
|                                    | Prog       | Peak  | Retro   |                              | Prog   | Peak   | Retro  |
| Grt                                |            | ~Alm <sub>56</sub> GrS <sub>29</sub> Prp <sub>13</sub> Sps <sub>2</sub><br>inclusions of Omp,<br>Qtz, Ap, Mag, Am | Slight resorption                                       | Grt                          | Alm <sub>48</sub> Prp <sub>14</sub> GrS <sub>30</sub> Sps <sub>2</sub> | Alm <sub>53</sub> Prp <sub>17</sub> GrS <sub>29</sub> Sps <sub>1</sub>           | Minor resorption   |
| Cpx                                |            | Omp Di/Hd <sub>60</sub> Jd <sub>32</sub> Aeg <sub>8</sub><br>Tiny Grt inclusions                                  | ~Di/Hd <sub>75</sub> Jd <sub>13</sub> Aeg <sub>12</sub> | Cpx                          |  | Omp relics in matrix,<br>(Di+Hd) <sub>60</sub> Jd <sub>32</sub> Aeg <sub>3</sub> | (Di+Hd) <sub>80</sub> Jd <sub>17</sub> Aeg <sub>3</sub> ,<br>symplectite                     |
| Rt                                 |            |   |   | Rt                           |  |  |  |
| Qtz                                |            |   |   | Phg                          |  |  | ?  |
| Ep/Zo                              |            |   |   | Qtz                          | ?  |  |  |
| Mag                                | .....      |   | .....   | Am                           |  |  | Poikiloblastic pargasite   |
| Am                                 | Blue-Green |   | Poikiloblastic<br>magnesirotaramite                     | Pl                           | .....?   |  | Ab <sub>85</sub>   |
| Pl                                 | .....?     |   | Poikiloblastic<br>Ab <sub>91</sub>                      | Ttn                          |  |  |  |
| Ttn                                |            |   | Rt cores  |                              |  |  |  |

935 K, but crystals of the HP assemblage are larger (up to 2 mm) and the rock was retrogressed more (Figure 5). The eclogite-facies assemblage includes Grt + Omp + Rt + Qtz + Ep + Mag and accessory Ap + Zrn (Table 2). Garnet has minor patchy zoning; its composition is ca. Alm<sub>56</sub>GrS<sub>29</sub>Prp<sub>13</sub>Sps<sub>2</sub> and Fe# = 0.80 (Figures 6 and 7; Supplementary Table 1). Close to omphacite inclusions, garnets have Fe# = 0.86 possibly due to retrogression exchange reactions. The composition of omphacite as inclusion in garnet and as idioblastic grains is Di/Hd<sub>60</sub>Jd<sub>32</sub>Aeg<sub>8</sub> (Supplementary Table 2). The composition near the grain boundaries and in strongly resorbed grains is higher in Aeg and Di components, with composition near Di/Hd<sub>75</sub>Jd<sub>13</sub>Aeg<sub>12</sub> (Figure 8). The retrograde assemblage includes poikiloblastic albite (Ab<sub>91</sub>) and magnesirotaramite.

Sample 935 RI is a gneiss containing Am, Grt, Qtz, Pl, Czo, Cb, Bt, Ttn, and Wmca. (Table 2). Relict HP phases include xenoblastic omphacite and cores of rutile in titanite. Randomly oriented biotite flakes grew as the

latest phase (Figure 5). The garnet inner core is Alm<sub>54</sub>Prp<sub>11</sub>GrS<sub>34</sub>Sps<sub>1</sub> and Fe# varies unsystematically in the range 0.75–0.78. We interpret this composition to best preserve the HP garnet. The outer 100–200 μm is Alm<sub>58</sub>Prp<sub>13</sub>GrS<sub>28</sub>Sps<sub>1</sub> with Fe# = 0.75 (Supplementary Table 1), a composition interpreted to have been produced by the intense amphibolite-facies overprint. Clinopyroxene is poorly preserved, mostly as symplectite. The composition corresponds to omphacite with (Di+Hd)<sub>73</sub>Jd<sub>24</sub>Aeg<sub>3</sub> (Supplementary Table 2), which reflects partial retrogression after the HP event (Figure 8). Phengite contains up to 3.37 Si apfu, with interlayer cations X<sub>Ca</sub><0.01, X<sub>Na</sub> = 0.03–0.11, and X<sub>K</sub> = 0.89–0.96. Retrograde amphibole is magnesirotaramite (Figure 9). Plagioclase composition is homogeneous Alb<sub>89–90</sub>An<sub>10–11</sub>Or<sub><0.5</sub>.

Eclogite sample 935S bears the assemblage Grt + Omp + Rt + Phg + Qtz, which was partially overprinted by Am + Pl + Wmca? + Bt + Ttn + Qtz (Table 2). The rock's foliation is defined by millimetre-scale compositional

**Table 3.** Mineral parageneses of sample series 887 (Agua Caliente eclogite), sample 728 (Cubulco amphibolite), and sample series 659 (Tuncaj eclogite) during prograde, peak, and retrogression stages of metamorphism, including key petrographic features and mineral compositions.

| Agua Caliente, samples 887a-b   |  |   | Cubulco Amphibolite, sample 728  |  |      |   |   |
|---------------------------------|--|---|--|--|------|---|---|
|                                 | Prog   | Peak  | Retro  |  | Prog | Peak (epidote-amphibolite)                            | Retro   |
| Cpx                             |  | Omp<br>cores up to Jd <sub>32</sub>   | Di symplectite near<br>Am  |  |      |   |   |
| Wmca                            |  | Finer, define fabric  | - Coarser, random  |  | Am   | Mineral lineation,<br>magnesian-hornblende            |   |
| Grt                             |  | Alm <sub>51-55</sub> Gr <sub>29-34</sub> Prp <sub>8-11</sub> Sps <sub>5-7</sub> , inclusions of<br>Omp      |  |  | Pl   | Ab <sub>98</sub>                                      |   |
| Rt                              |  |   | Rimmed by Ttn  |  | Czo  | Fine, Ps <sub>0.10-0.13</sub>                         |   |
| Czo                             |  |   | Ps <sub>0.21</sub>   |  | Wmca | Phg 3.35 Si   |   |
| Pl                              |  |   | Ab <sub>92</sub> , Poikiloblastic  |  | Bt   |   |   |
| Am                              |  |   | Poikiloblastic   |  | Chl  | Cores in Bt   |   |
| Ttn                             |  |   | Rt cores   |  | Grt  | Alm <sub>49</sub> Prp <sub>16</sub> Sps <sub>16</sub> | Alm <sub>55</sub> Prp <sub>10</sub> Sps <sub>10</sub> |
| Bt                              |  |   |  |  | Ttn  | Clusters  |   |
|                                 |  |   |  |  | Hem  |   |   |
|                                 |  |   |  |  |      |   |   |
| Tuncaj Eclogite, samples 659a-b |  |   |  |  |      |   |   |
|                                 | Prog   | Peak  | Retro  |  |      |   |   |
| Grt                             | Core, ttn inclusion<br>Alm <sub>40-45</sub> Gr <sub>50</sub> Prp <sub>13</sub><br>Sp <sub>17</sub> | Rim, Omp + Czo +<br>Amp inclusions,<br>Alm <sub>50</sub> Gr <sub>33</sub> Prp <sub>9</sub> Sps <sub>1</sub> | Alm <sub>52</sub> Gr <sub>37</sub> Prp <sub>8</sub> Sps <sub>3</sub> ,<br>resorbed |  |      |   |   |
| Cpx                             |  | Jd <sub>33-45</sub> (Di+Hd) <sub>52-66</sub> Aeg <sub>6-10</sub>  | Symplectite  |  |      |   |   |
| Ttn                             | Tiny inclusions  | ?   |  |  |      |   |   |
| Czo + Zo                        |  | Ps <sub>0.05</sub> and Ps <sub>0.1-0.13</sub>   |  |  |      |   |   |
| Am                              |  | Ferropargasite<br>inclusions in Grt rims  | sodic ferropargasite,<br>magnesian hornblende to<br>barroisite                     |  |      |   |   |
| Pl                              |  |   | Ab <sub>98</sub>   |  |      |   |   |

banding. Late amphibole is poikiloblastic (Figure 5). Garnet is subidioblastic and weakly zoned concentrically (Figure 7) with inner cores Alm<sub>48</sub>Prp<sub>14</sub>Gr<sub>36</sub>Sps<sub>2</sub> mantled by Alm<sub>53</sub>Prp<sub>17</sub>Gr<sub>29</sub>Sps<sub>1</sub> and outermost rims Alm<sub>53</sub>Prp<sub>18</sub>Gr<sub>27</sub>Sps<sub>2</sub> (Figure 6; Supplementary Table 1). Clinopyroxene occurs as relict grains in the matrix or forming symplectite with plagioclase. Matrix clinopyroxene composition ranges from ca. (Di+Hd)<sub>60</sub>Jd<sub>37</sub>Aeg<sub>3</sub> (Supplementary Table 2) to ca. (Di+Hd)<sub>80</sub>Jd<sub>17</sub>Aeg<sub>3</sub> in the rims (Figure 8). The composition of most analysed amphiboles corresponds to pargasite (Figure 9). Plagioclase has a nearly homogeneous composition of Alb<sub>84-87</sub>An<sub>12-15</sub>Or<sub>01</sub>.

## 6.2. Gneiss-hosted eclogites at Agua Caliente River

Samples 407, 887a, and 887b are phengite-bearing eclogite retrogressed to amphibolite with poikiloblastic amphibole and plagioclase (Figure 5). The peak-pressure assemblage comprises <0.4 mm crystals of Omp + Wmca + Grt + Rt + Czo (in order of abundance; Table 3). Garnet zoning is patchy and has a compositional range of

Alm<sub>51-55</sub>Gr<sub>29-34</sub>Prp<sub>8-11</sub>Sps<sub>5-7</sub> and Fe# = 84–86 (Figures 6 and 7; Supplementary Table 1). The cores of coarser omphacite grains contain the highest Jd component of up to 32 mol%. Omphacite inclusions in garnet and some well-preserved crystals have compositions close to (Di+Hd)<sub>65</sub>Jd<sub>25-30</sub>Aeg<sub>5-10</sub> (Supplementary Table 2). Diopsidic pyroxenes also occur as part of very resorbed crystals within the plagioclase and in symplectite (Figure 8). The rocks contain two generations of white mica (Table 3). Rutile is partially rimmed by titanite and is best preserved as inclusions in white mica and omphacite. Retrograde amphibole and plagioclase are poikiloblastic and up to 3 cm long. Plagioclase is albite with composition Ab<sub>91-93</sub>. Amphibole composition is at the boundary between magnesian-taramite/pargasite and taramite/ferropargasite. Epidote (Ps<sub>0.21</sub>) is rare and mostly associated with plagioclase.

## 6.3. Northernmost occurrence of eclogite associated with serpentinites at Tuncaj

Samples of the 659 series represent the coherent metamorphic bodies >100 m long associated with even larger

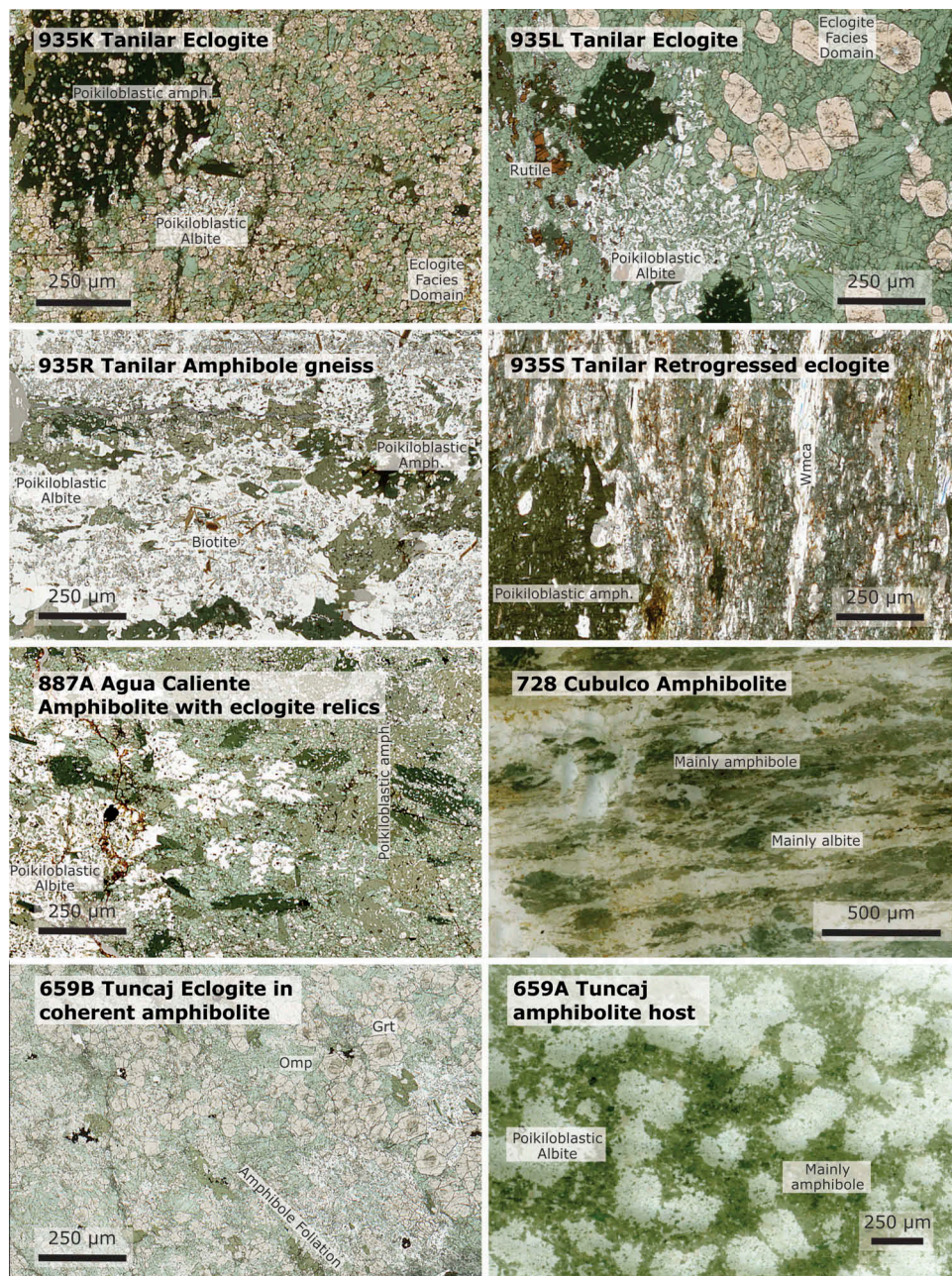


**Figure 5.** Scanned thin sections of representative analysed eclogites and amphibolites of the Sierra de Chuacús. Samples of the 935 and 887 series are partially amphibolitized eclogites hosted in orthogneiss of the Chuacús Complex; notice the contrast between the fine granoblastic eclogite-facies domains and the poikiloblastic retrogression domains. Sample 728 is the northernmost amphibolite occurrence in the Chuacús Complex, which is devoid of eclogitic relics. Samples of the 659 series represent the eclogite (B) domains in large, mappable, poikiloblastic amphibolite (A).

serpentinite bodies at Tuncaj (Figure 2). Eclogite sample 659b is from a decimetre- to metre-scale domain within the amphibolite. The sample contains the assemblage Grt + Omp + Ttn + Czo + Zo with minor retrograde Am + Pl (Figure 5; Table 3).

Garnet contains two growth zones: cores contain abundant but minuscule titanite, whereas the outer portions contain a few inclusions of Omp, Czo, and rare Am (ferropargasite). Core composition is  $\text{Alm}_{40-45}\text{Grs}_{40}\text{Prp}_{<3}$

$\text{Sps}_{\leq 17}$  (Figure 6). The boundary between the inclusion-rich core and the inclusion-poor garnet rim is an ca. 5  $\mu\text{m}$ -thick ring rich in grossular (Figure 7). The inclusion-poor rim of garnet with the lowest Sps has the composition  $\text{Alm}_{56}\text{Grs}_{33}\text{Prp}_9\text{Sps}_1$  and is interpreted to reflect peak eclogite-facies conditions. Unlike garnet, omphacite crystals exhibit patchy zoning. Most analyses correspond to  $\text{Jd}_{33-45}(\text{Di}+\text{Hd})_{52-66}\text{Aeg}_{<6}$  (Supplementary Table 2). The sample contains both Zo and Czo with compositions of

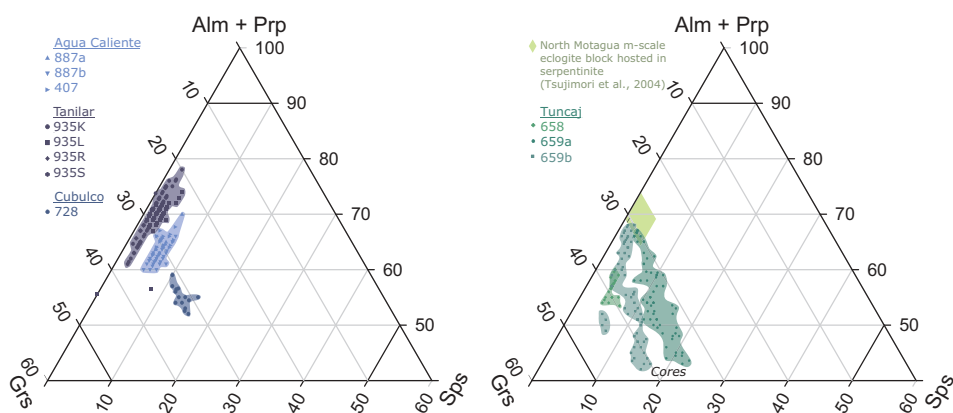


**Figure 6.** Garnet composition of the analysed samples in the Alm+Prp–Grs–Sps ternary diagram. Groups as in text.

$Ps_{<0.05}$  and  $Ps_{0.1-0.15}$ , respectively. The retrogression assemblage is characterized by albite ( $Ab_{98}$ ) and sodic ferropargasite.

Amphibolite sample 659a, collected ca. 20 m from the eclogite sample described above, is the most representative for the bulk of the Tuncaj outcrop. The rock is massive and is characterized by equant albite poikiloblasts and random aggregates of green magnesiohornblende-barroisite; both are associated with partially resorbed garnet. Titanite and minor epidote occur in the matrix.

Similar to garnet in Tuncaj eclogite, the garnet cores contain abundant tiny titanite inclusions, whereas rims have few or no inclusions. Some garnets show core inclusions that are aligned or form an S pattern, attesting to prior prograde foliation. The zoning pattern is bell-shaped in the core, reflecting partial preservation of prograde zoning. The composition of cores changes systematically from  $Alm_{41}Grs_{34}Prp_2Sp_{523}$  to  $Alm_{55}Grs_{31}Prp_4Sp_{510}$  in the garnet mantle. The maximum Fe# is  $0.93 \pm 0.02$  in the core and mantle (Figure 7) and 0.8 at the outermost rim. The largest analysed garnet shows a zoning pattern similar to garnet in Tuncaj eclogite (Figures 6 and 7). However, due to resorption, some rims with this composition were not preserved (Figure 7).

#### 6.4. Metamorphism of mafic protoliths in the northern flank of the Sierra de Chuacús

Overall, metamorphic grade in the Chuacús Complex decreases northward (van den Boom 1972). The northernmost occurrence of metamafic rocks rich in amphibole is in the hills around Cubulco (Figure 2), where bands of strongly lineated amphibolite are exposed. These amphibolites (sample 728; Figure 5) contain green amphibole, plagioclase, epidote, titanite, white mica, biotite, and rare garnet (Table 3). Similar

epidote-rich amphibolites were found 1.5 km E–SE of Cubulco; they share similar characteristics and do not contain relict eclogite-facies minerals. Cobbles from streams on the northernmost slopes of the Sierra de Chuacús near Cubulco and Rabinal also do not contain relict omphacite.

Unlike mafic rocks in the southern Sierra de Chuacús, Cubulco amphibolites exhibit a strong mineral lineation and not a poikiloblastic texture (Figure 5). Their amphibole is green edenite and magnesio-hornblende (ca. 60%) (Figure 9). Albitic plagioclase (ca. 20%) has a homogenous composition of  $Ab_{98\pm 1}$  and fine-grained clinozoisite (ca. 15%) has composition  $Ps = 0.10-0.13$ . Very fine-grained titanite occurs as lens-shaped aggregates. Rare biotite contains cores of prograde chlorite. Small, randomly oriented white mica crystals are phengite with up to 3.35 Si apfu (11 O basis). Scarce garnet (ca. 2%) occurs in a millimetre-wide band. Garnet crystals are weakly zoned with a core composition of  $Alm_{49}Prp_{03}Sp_{515}$  and rims of  $Alm_{54}Prp_{05}Sp_{510}$  (Figure 7). The presence of scarce and zoned garnet and the association of hornblende and albite are typical of the epidote-amphibolites facies (e.g. Apter and Liou 1983), conditions indicative of the greenschist- to amphibolite-facies transition at relatively high pressure. Importantly, this sample has no relics of an earlier eclogite-facies assemblage.

#### 6.5. Thermobarometry

Two *in situ* Tanilar eclogites (935 R and 935S) yielded nearly identical univariant thermometry curves. One phengite-bearing sample yielded conditions of  $P \approx 2.7$  GPa and  $T \approx 750^\circ\text{C}$  (Figure 10), which are very close to the coesite stability field. Similar but slightly lower pressure conditions were obtained for the group of phengite-bearing eclogites from Río Agua Caliente, which yielded  $T = 720-790^\circ\text{C}$  and  $P = 2.1-2.5$  GPa. Assuming an overburden with a mean density of  $3.2 \times 10^3$  kg/m<sup>3</sup>, which is reasonable for the

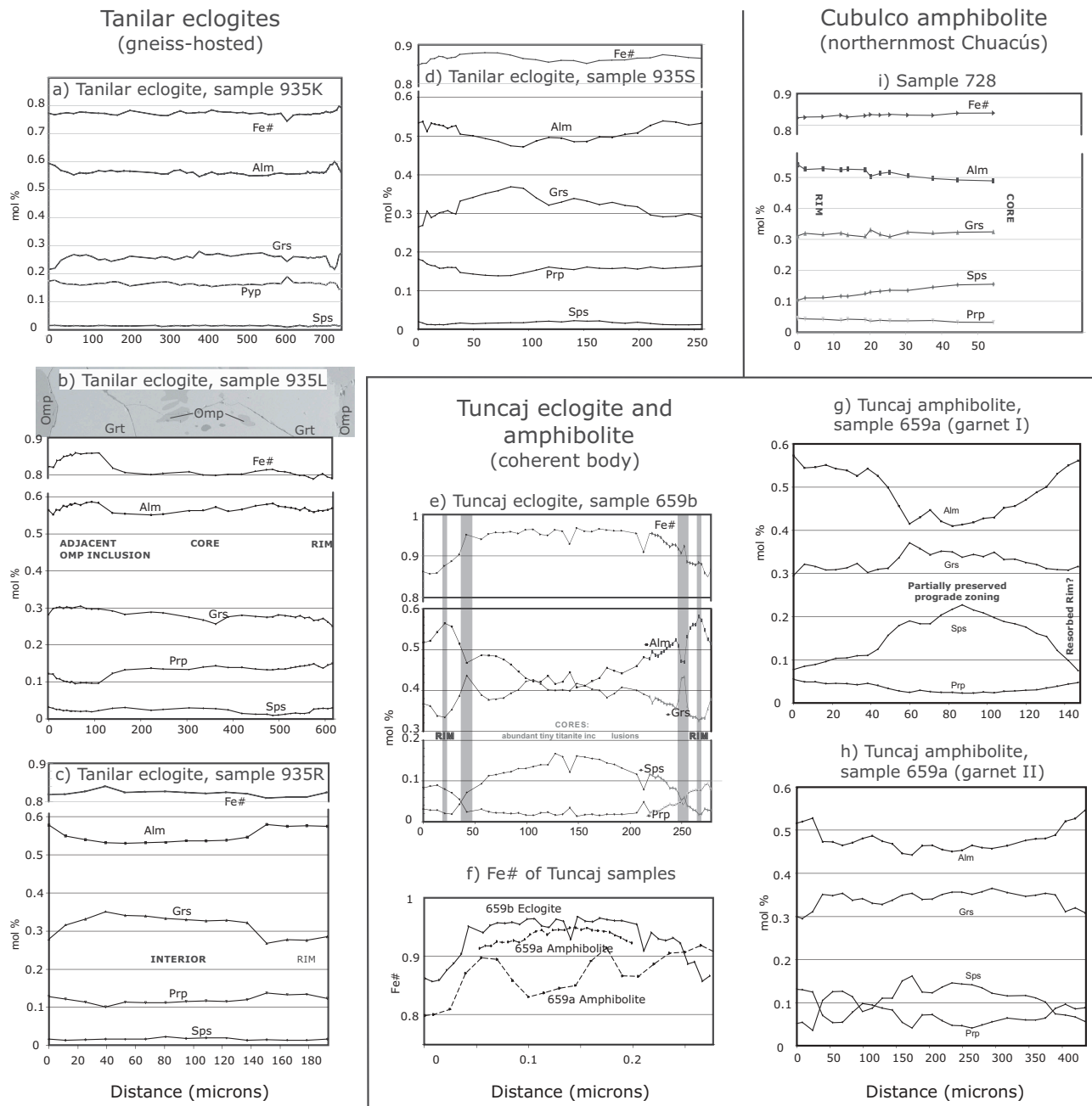


**Figure 7.** Rim-to-rim garnet zoning of Tanilar, Cubulco, and Tuncaj eclogites and amphibolites, expressed as Alm, Prp, Grs, Sps apfu, and Fe#.

Caribbean lithosphere (see below), these conditions correspond to a mantle depth of ca. 80 km. The Grt–Cpx thermometer applied to the two eclogite cobbles collected from the gorge of the Tanilar River (935 K and 935 L) yielded consistent results; at the plausible  $P = 2.0\text{--}2.6$  GPa range, the estimated  $T = 790\text{--}830^\circ\text{C}$  is higher than in other samples. The Tuncaj eclogite seems to have equilibrated at a lower temperature when compared to gneiss-hosted eclogite. The univariant curves for Grt + Cpx thermometry in the  $P = 1.5\text{--}2.5$  GPa range yield  $T = 680\text{--}720^\circ\text{C}$ .

## 7. Discussion

The variety of eclogites in the GSC is greater than previously realized. Based on field occurrence, lithologic association, mineral parageneses, and structure, we recognized, from the south to the north, metre-scale blocks of lawsonite-eclogite hosted in serpentinite south of the Motagua Fault (e.g. Tsujimori *et al.* 2005, 2006a), similarly sized blocks of epidote eclogite hosted in serpentinite mélangé north of the Motagua Fault (e.g. Harlow 1994), coherent bodies up to hundreds of metres long of eclogite extensively retrogressed to

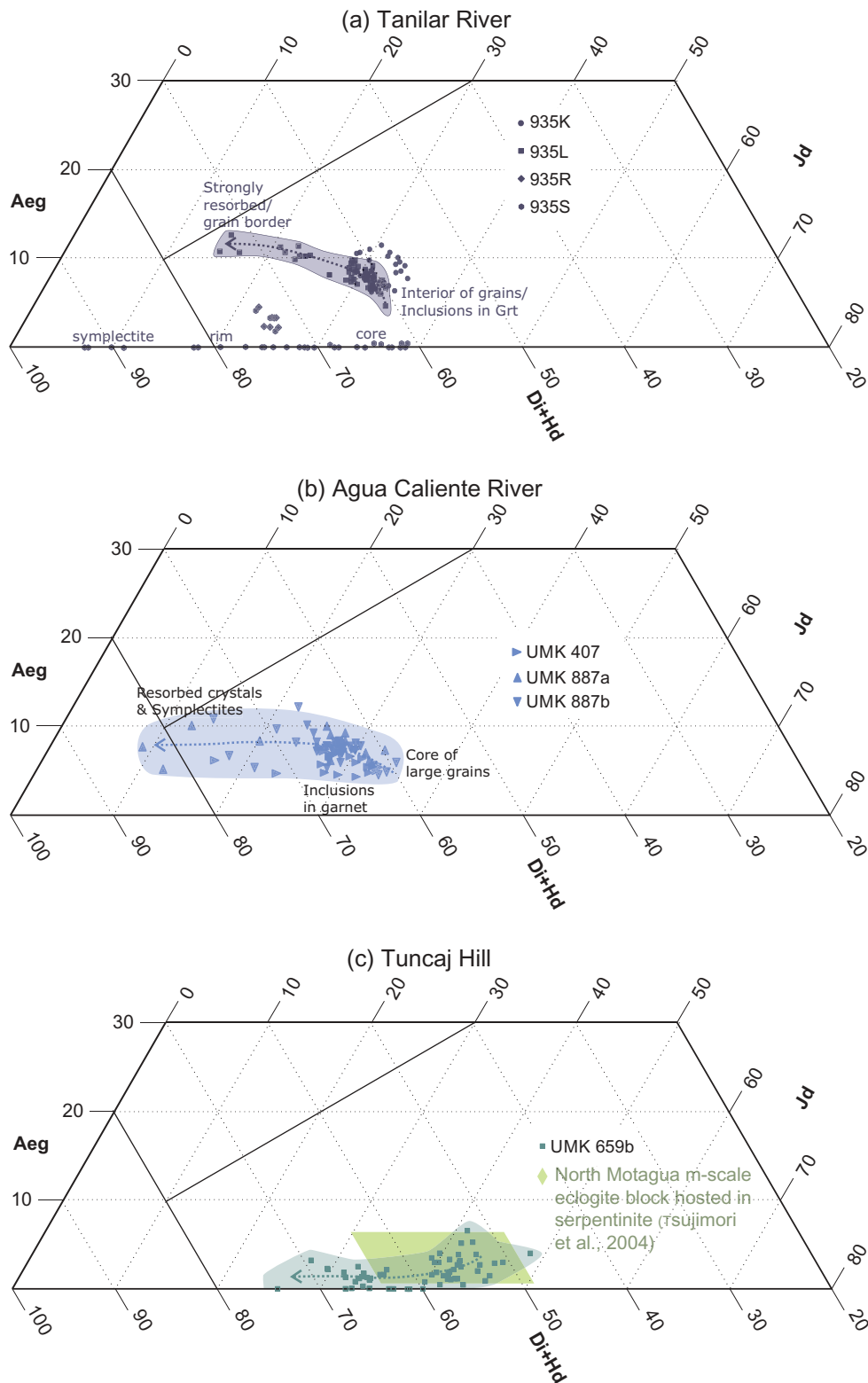


**Figure 8.** Clinopyroxene composition of the Tanilar River, the Agua Caliente River, and the Tuncaj Hill eclogites based on Morimoto (1988).  $\text{Fe}^{3+}$  calculated as  $\text{Na} - \text{Al} - \text{Cr} - 2\text{Ti}$ .

amphibolite (e.g. Tuncaj and La Canoa; Figure 2), and eclogites as bands and lenses hosted in quartzofeldspathic gneisses with continental affinity of the Chuacús

Complex (e.g. Ortega-Gutiérrez *et al.* 2004; Martens *et al.* 2012). All these eclogite varieties are an integral part of the GSC (Table 1).

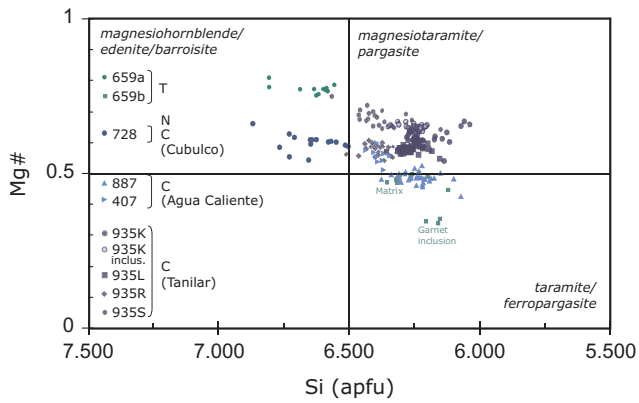


**Figure 9.** Compositions of retrogression amphiboles in the Si (apfu) versus Mg# space.

### 7.1. Mexican origin of the southern lawsonite eclogite

The subduction zone where southern lawsonite eclogites crystallized under near-forbidden zone  $P$ – $T$  conditions was very cold, implying a prolonged process of refrigeration by long-lived subduction. This feature contrasts with Ratschbacher *et al.*'s (2009) proposition of lawsonite eclogite formation in a very young and short-lived subduction zone.

Jadeitite formation from aqueous subduction fluids (P-type) or metasomatism (R-type) occurred in the Late

Jurassic (Fu *et al.* 2009; Tsujimori and Harlow 2012; Flores *et al.* 2013) and oceanic mafic protolith recrystallized at HP conditions in the Early Cretaceous (Sm–Nd mineral isochron age of an eclogite ca. 132 Ma; Brueckner *et al.* 2009). The above-mentioned features preclude origin in a Caribbean subduction zone because the time of initiation of the Great Caribbean arc is too young, at ca. 135 Ma (Rojas-Agramonte *et al.* 2011; Pindell *et al.* 2011). A more plausible initial locus for these eclogites was offshore Western Mexico, where Farallon subduction was producing arc rocks in the Guerrero terrane (Mortensen *et al.* 2008; Martini *et al.* 2014; Figure 11), contemporaneous with South Motagua jadeitite and eclogite formation. The latest Jurassic U–Pb age of southern jadeitite may indicate early hydrothermal processes produced by dehydration of the newly established slab in the Guerrero domain, contemporaneous with the opening of the Arperos back arc (e.g. Martini *et al.* 2011).

### 7.2. Caribbean origin of North Motagua eclogites

Serpentinite-hosted eclogites north of the Motagua Fault equilibrated at higher temperatures than those in the south, yet their ages are roughly analogous (Brueckner *et al.* 2009). When only Sm–Nd ages with

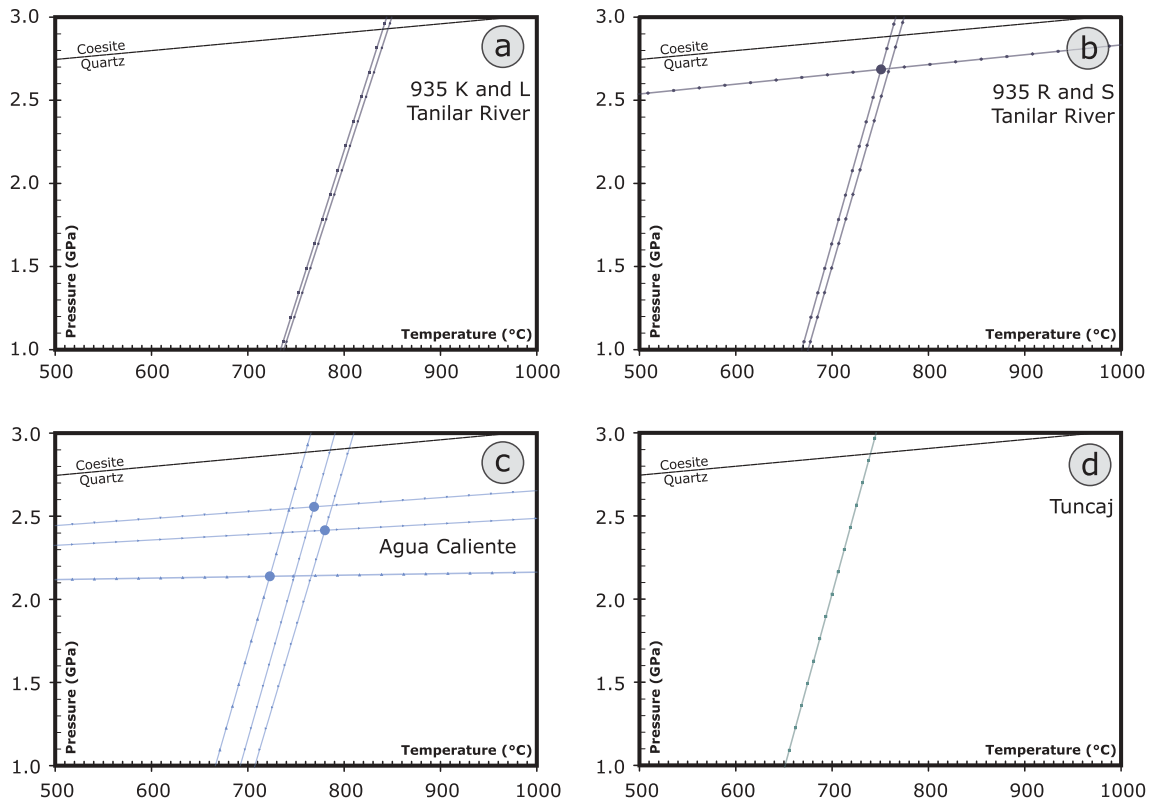


**Figure 10.** Calculated curves in  $T$  versus  $P$  space of the Tanilar River, the Agua Caliente River, and the Tuncaj Hill eclogites based on  $\text{Fe}^{2+}$ –Mg exchange and the Grt–Cpx–Wmca barometer after Krogh Ravna and Terry (2004).

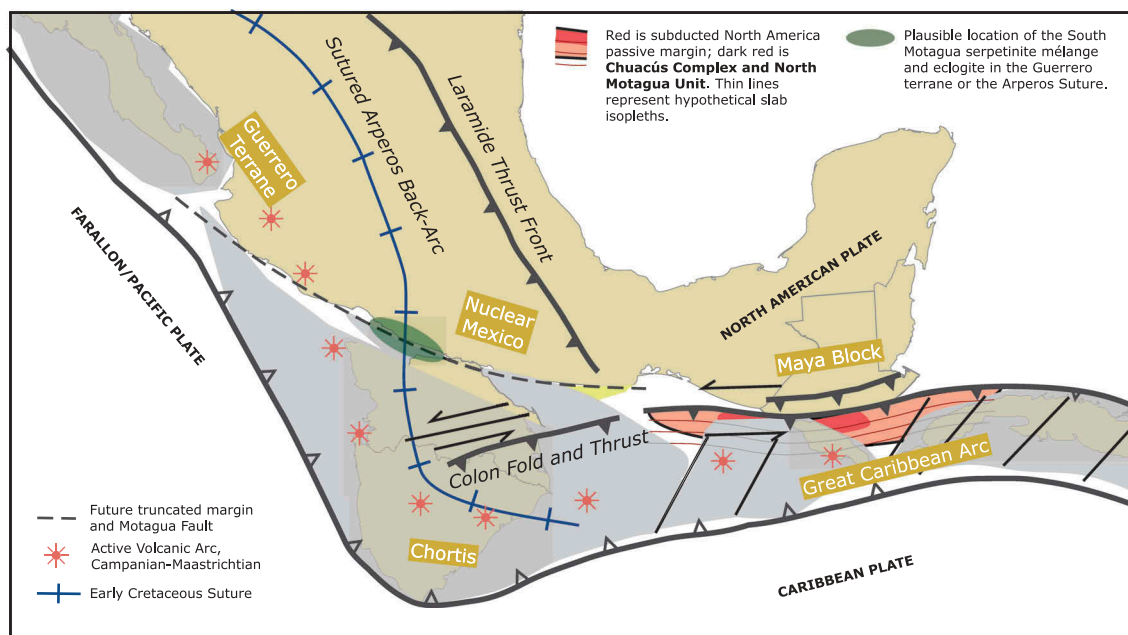


**Figure 11.** Schematic Campanian–Maastrichtian palaeotectonic reconstruction of the southern North America margin and the Great Caribbean Arc with elements taken from Rogers *et al.* (2007), Pindell and Kennan (2009), and Ratschbacher *et al.* (2009). Notice how the passive margin of North America is subducted underneath the Jamaica and Western Cuba parts of the Great Caribbean Arc.

MSWD <2 are considered, the age range is 137–118 Ma. A tectonic setting in a Farallon subduction but in a position within a hotter isotherm is therefore also plausible. However, such a model is very complex because it requires tectonic transport along the northern Chortis (Figure 11) from Mexico to Central America and the transference of eclogites and associated ultramafics to a position north of the Motagua Fault by transpression or tectonic anastomosing along the plate boundary (e.g. Brueckner *et al.* 2009).

A simpler model is to consider an origin in a subduction zone under the Great Caribbean Arc. The above age range for northern eclogite blocks is consistent with an origin from young and relatively hot proto-Caribbean subduction, which also explains the relatively higher temperatures recorded in the northern epidote eclogites. We prefer this model because transference of the North Motagua Unit from the Great Caribbean lithosphere (hanging wall) to the Maya Block (North America) is easily explained by the Late Cretaceous collision of the arc with the southern passive margin of North America.

Eclogite also occurs as relics in coherent bodies of amphibolite in the oceanic North Motagua Unit (Figure 2). An example is the Tuncaj eclogite that preserved a two-stage prograde evolution with the peak assemblage Grt + Omp + Ttn + Czo + Zo ± Am, which reached temperatures <720°C, lower than the Chuacús eclogites but slightly higher than the northern blocks in serpentinite melange. This feature is consistent with the

better preservation of prograde zoning in garnet. Peak Cpx composition contains up to 47 mol% Jd molecule and mostly <5 mol% Aeg. These bodies are interpreted as relatively large blocks of oceanic crust that were subducted and metamorphosed to the eclogite facies, and then accreted to the Caribbean plate.

We surmise that the two varieties of eclogite in the North Motagua Unit were probably produced in the same subduction zone inasmuch as they are associated with similar serpentinite units. Large coherent bodies preserved their structural integrity during subduction, whereas the smaller metre-scale blocks represent the most sheared portions of similar subducted lithosphere in the subduction channel. Importantly, a two-stage garnet growth is present in both and their peak Cpx and Grt compositions are analogous (Figure 6; Figure 8).

### 7.3. Late Cretaceous continental subduction of the Chuacús Complex

Eclogites in the Tanilar unit of the sialic Chuacús Complex are characterized by the peak paragenesis Omp + Grt + Rt ± Wmca ± Qtz ± Ep. Overall Grt composition ranges Alm<sub>50–60</sub>Prp<sub>10–20</sub>GrS<sub>20–40</sub> with minor Mn component. Prograde compositional zoning is not pronounced, consistent with the relatively high-temperature eclogite-facies recrystallization at 720–830°C. Cpx composition evolved from Omp with up to 35 mol% Jd and <10 mol% Aeg at the peak stage to retrograde diopside mostly as symplectite. Phengite-

bearing eclogites allowed constraining  $P = 2.1\text{--}2.7$  GPa, near but below the stability field of coesite. Previous U–Pb zircon geochronology has shown that the eclogite-facies event took place during the Late Cretaceous (Campanian; Martens *et al.* 2012).

The Chuacús eclogites are interpreted to represent the continental subduction of North America's passive margin as it reached the Great Caribbean trench (Figure 11). This was the same subduction zone where the North Motagua Unit eclogites had been formed from the previously subducted proto-Caribbean crust ca. 40–50 Ma earlier. Continental crustal materials of the Chuacús Complex may have been carried to more than ca. 80 km, a mantle depth within the stability field of coesite. Perhaps only HP-recrystallized portions were exhumed, and hence no coesite has been conclusively identified in Chuacús eclogites (e.g. Ortega-Gutiérrez *et al.* 2004).

#### 7.4. Retrogression of HP belts north of the Motagua Fault

The short time span between the formation of Chuacús eclogite at ca. 76 Ma and the cooling ages of ca. 74 Ma or slightly younger shows that the metamorphic path of Chuacús eclogites does not reflect a continuous process of subduction that proceeded for many millions of years, but a relatively short-lived process with rapid exhumation. We envision that the Chuacús slab was unstable at mantle depth, triggering either slab break-off or delamination of part of the sialic crust from the continental lithosphere. We propose that during this process the Chuacús block carried pieces of accreted oceanic lithosphere of the hanging wall on its way from the mantle to mid-crustal depths. This is how North Motagua serpentinite, serpentinite mélangé with exotic blocks, and coherent blocks of eclogite accreted to the hanging wall were first juxtaposed to the sialic Chuacús.

Once exhumed to crustal depths, the Chuacús Complex and the North Motagua Unit were coevally retrogressed in the Campanian-Maastrichtian at similar epidote-amphibolite conditions. This process involved the decompression melting of the sialic unit producing pegmatites that intruded both the Chuacús and the North Motagua units and the release of abundant fluids that facilitated retrogression reactions producing poikiloblastic epidote-amphibolites.

#### 7.5. How far north of the Motagua Fault does the Guatemala Suture reach?

Finally, we want to address three related but different questions, namely how far north do eclogites (sensu-

stricto) occur in the Sierra de Chuacús, how far north can eclogite-facies conditions be traced, and how far north HP assemblages are present in the suture in general.

Our field and petrologic study has shown that, unlike Chuacús eclogite, mafic protoliths in the Rabinal–Cubulco area to the north (Figure 2) underwent peak conditions at epidote-amphibolite facies and do not contain eclogite relics. Still further north of the Rabinal–Cubulco area, there are mafic enclaves in the sheared granites that contain a greenschist-facies assemblage of albite + chlorite + epidote + quartz + titanite ± actinolite. Amphibolites immediately south of Rabinal are rich in epidote but do not contain relics of an eclogite-facies assemblage. In fact, sensu-stricto eclogites in the northern flank of the Sierra de Chuacús are rare, if they are present at all. Here, we want to emphasize that considering an amphibolite to be a retrograde eclogite merely due to the presence of abundant garnet is not conclusive (c.f. Ortega-Gutiérrez *et al.* 2007). Provided what is currently known, we also conclude that the northernmost occurrence of eclogite in the GSC is the Cerro Tuncaj outcrop (Figure 2).

The northern boundary of the exhumed sialic block that contains eclogite-facies assemblages is yet to be determined. However, the boundary of eclogite-facies conditions must lie south of the amphibolites devoid of eclogitic relics at Cubulco and Rabinal, and north of the gneisses at Ixchel (same latitude as Tuncaj Hill; Figure 2). We therefore surmise that the boundary in question is located in the northern flank of the Sierra, in contrast to proposals that regard the BVSZ as the boundary. To better constrain this boundary, it will be helpful to establish the  $P$ – $T$  conditions of the widespread metapelites (Figure 2), particularly of those rich in Cld and devoid of Bt, which suggest HP conditions, perhaps in the eclogite-facies field (e.g. El-Shazly and Liou 1991).

Finally, we address how far north an HP gradient is registered in Central Guatemala. HP metamorphism has imprinted not only mafic high-grade rocks of the Chuacús Complex described in this article, but also granitic and metasedimentary rocks within the BVSZ (e.g. Ortega-Obregón 2005). Despite the metamorphic grade being considerable lower in the shear zone, metamorphic phengite composition in mylonitic granite is indicative of HP conditions (Solari *et al.* 2013). The northern boundary of the subducted HP slab is therefore the boundary of metamorphosed versus unmetamorphosed rocks shown in Figure 2.

#### Acknowledgements

We would like to express our gratitude to Robert Jones (Stanford University) for providing superb assistance in the

operation of the electron microprobe, to Antonio García-Casco at University of Granada for facilitating thin section preparation, to Rafael Torres de León and Carlos Ortega Obregón for assistance in the field study of Tuncaj eclogite, and to Lothar Ratschbacher and Fernando Ortega-Gutiérrez for the excellent discussions of Chuacús eclogites in the field. Yui Tzen-Fu, Luigi Solari, and Hannes Brueckner are thanked for reviewing the manuscript and providing very useful feedback. Finally, our sincere gratitude to Sorena Sorensen for her enlightening contributions to the understanding of the geologic processes recorded in the Guatemala Suture Complex and initial support for our NSF proposal. This research was supported by NSF EAR# 0510325, Stanford University, and in part by the MEXT/JSPS KAKENHI (15H05212) to T. Tsujimori.

## Disclosure statement

No potential conflict of interest was reported by the authors.

## Funding

This work was supported by the NSF [EAR# 0510325]; Stanford University; Ministry of Education, Culture, Sports, Science, and Technology/ Japan Society for the Promotion of Science KAKENHI [15H05212].

## ORCID

Tatsuki Tsujimori  <http://orcid.org/0000-0001-9202-7312>

## References

- Apted, M.J., and Liou, J.G., 1983, Phase relations among greenschist, epidote amphibolite, and amphibolite in a basaltic system: *American Journal of Science*, v. 283A, p. 328–354.
- Baumgartner, P.O., Flores, K., Bandini, A.N., Girault, F., and Cruz, D., 2008, Upper Triassic to Cretaceous radiolaria from Nicaragua and northern Costa Rica-The Mesquito composite oceanic terrane: *Ophioliti*, v. 33, p. 1–19.
- Beccaluva, L., Bellia, S., Coltorti, M., and Dengo, G., 1995, The northwestern border of the Caribbean plate in Guatemala: New geological and petrological data on the Motagua ophiolitic belt: *Ophioliti*, v. 20, p. 1–15.
- Bertrand, J., and Vuagnat, M., 1975, Sur la présence de basaltes en coussins dans la zone ophiolitique méridionale de la Cordillere Centrale du Guatemala: *Bulletin Suisse De Minéralogie Et Pétrographie*, v. 55, p. 136–142.
- Bertrand, J., and Vuagnat, M., 1976, Etude pétrographique de diverses ultrabasites ophiolitiques du Guatemala et de leurs inclusions: *Bulletin suisse de minéralogie et pétrographie*, v. 56, p. 527–540.
- Bertrand, J., and Vuagnat, M., 1977, Données chimiques diverses sur les ophiolites du Guatemala: *Bulletin suisse de minéralogie et pétrographie*, v. 57, p. 466–483.
- Bertrand, J., and Vuagnat, M., 1980, Inclusions in the serpentinite mélangé of the Motagua Fault Zone, Guatemala, *in* Proceedings of the international symposium on tectonic inclusions and associated rocks in Serpentinites, Geneva: *Archives De Sciences*, v. 33, p. 321–335.
- Blanco-Quintero, I.F., Rojas-Agramonte, Y., García-Casco, A., Kröner, A., Mertz, D.F., Lázaro, C., Blanco-Moreno, J., and Renne, P.R., 2011, Timing of subduction and exhumation in a subduction channel: Evidence from slab melts from La Corea Mélange (eastern Cuba): *Lithos*, v. 127, p. 86–100. doi:10.1016/j.lithos.2011.08.009
- Bonis, S., 1993, Mapa geológico de Guatemala 1:250,000. ND-15-8-G: Guatemala, Instituto Geográfico Militar.
- Bonis, S., Bohnenberger, O.H., and Dengo, G., 1970, Mapa geológico de la República de Guatemala 1:500,000: Guatemala, Instituto Geográfico Nacional.
- Brueckner, H.K., Avé Lallemant, H.G., Sisson, V.B., Harlow, G.E., Hemming, S.R., Martens, U., Tsujimori, T., and Sorensen, S.S., 2009, Metamorphic reworking of a high pressure–low temperature mélangé along the Motagua fault, Guatemala: A record of Neocomian and Maastrichtian transpressional tectonics: *Earth and Planetary Science Letters*, v. 284, p. 228–235. doi:10.1016/j.epsl.2009.04.032
- Carswell, D., Wilson, R., and Zhai, M., 2000, Metamorphic evolution, mineral chemistry and thermobarometry of schists and orthogneisses hosting ultra-high pressure eclogites in the Dabieshan of central China: *Lithos*, v. 52, p. 121–155. doi:10.1016/S0024-4937(99)00088-2
- Carswell, D.A., O'Brien, P.J., Wilson, R.N., and Zhai, M., 1997, Thermobarometry of phengite-bearing eclogites in the Dabie mountains of central China: *Journal of Metamorphic Geology*, v. 15, p. 239–252. doi:10.1111/j.1525-1314.1997.00014.x
- Cawthorn, R.G., and Collerson, K.D., 1974, The recalculation of pyroxene end-member parameters and the estimation of ferrous and ferric iron content from electron microprobe analyses: *American Mineralogist*, v. 59, p. 1203–1208.
- Dengo, G., 1969, Problems of tectonic relations between Central America and the Caribbean: *Gulf Coast Association of Geological Societies*, v. 19, p. 311–320.
- Donnelly, T.W., Horne, G.S., Finch, R.C., and López-Ramos, E., 1990, Northern Central America; the Maya and Chortis blocks, *in* Dengo, G., and Case, J.E., eds., *The Caribbean region: Boulder, Colorado, Geological Society of America, The geology of North America*, v. H, p. 37–76.
- Droop, G.T., 1987, A general equation for estimating Fe<sup>3+</sup> concentrations in ferromagnesian silicates and oxides from microprobe analyses, using stoichiometric criteria: *Mineralogical Magazine*, v. 51, p. 431–435. doi:10.1180/minmag
- El-Shazly, A.K., and Liou, J.G., 1991, Glaucofan chloritoid-bearing assemblages from NE Oman: Petrologic significance and a petrogenetic grid for high P metapelites: *Contributions to Mineralogy and Petrology*, v. 107, p. 180–201. doi:10.1007/BF00310706
- Flores, K.E., Martens, U.C., Harlow, G.E., Brueckner, H.K., and Pearson, N.J., 2013, Jadeitite formed during subduction: In situ zircon geochronology constraints from two different tectonic events within the Guatemala Suture Zone: *Earth and Planetary Science Letters*, v. 371–372, p. 67–81. doi:10.1016/j.epsl.2013.04.015
- Fu, B., Valley, J.W., Kita, N.T., Spicuzza, M.J., Paton, C., Tsujimori, T., Bröcker, M., and Harlow, G.E., 2009, Multiple origins of zircons in jadeitite: Contributions to Mineralogy and Petrology, v. 159, p. 769–780. doi:10.1007/s00410-009-0453-y
- Ganguly, J., Chakraborty, S., Sharp, T.G., and Rumble, D., 1996, Constraint on the time scale of biotite-grade

- metamorphism during Acadian Orogeny from a natural garnet-garnet diffusion couple: *American Mineralogist*, v. 81, p. 1208–1216. doi:10.2138/am-1996-9-1019
- Giunta, G., Beccaluva, L., Coltorti, M., Mortellaro, D., Siena, F., and Cutrupia, D., 2002, The peri-Caribbean ophiolites: Structure, tectono-magmatic significance and geodynamic implications: *Caribbean Journal of Earth Science*, v. 36, p. 1–20.
- Guzmán-Speziale, M., Pennington, W.D., and Matumoto, T., 1989, The triple junction of the North America, Cocos, and Caribbean Plates: Seismicity and tectonics: *Tectonics*, v. 8, p. 981–997. doi:10.1029/TC008i005p00981
- Hamm, H.M., and Vieten, K., 1971, Zur Berechnung der kristall-chemischen Formel und des Fe<sup>3+</sup>-Gehaltes von Klinopyroxenen aus Elektronenstrahl-Mikroanalysen. *Neues Jahrbuch für Mineralogie: Stuttgart, Monatshefte*, 310–314 p.
- Harlow, G.E., 1994, Jadeitites, albitites and related rocks from the Motagua Fault Zone, Guatemala: *Journal of Metamorphic Geology*, v. 12, p. 49–68. doi:10.1111/jmg.1994.12.issue-1
- Harlow, G.E., Hemming, S.R., Lallemand, H.G.A., Sisson, V.B., and Sorensen, S.S., 2004, Two high-pressure–low-temperature serpentinite-matrix mélange belts, Motagua fault zone, Guatemala: A record of Aptian and Maastrichtian collisions: *Geology*, v. 32, p. 17–20. doi:10.1130/G19990.1
- Harlow, G.E., Sisson, V.B., Avé Lallemand, H.G., Sorensen, S.S., and Seitz, R., 2003, High-pressure, metasomatic rocks along the Motagua fault zone, Guatemala: *Ofoliti*, v. 28, p. 115–120.
- Holland, T.J.B., 1990, Activities of components in omphacitic solid solutions: *Contributions to Mineralogy and Petrology*, v. 105, p. 446–453. doi:10.1007/BF00286831
- Holland, T.J.B., and Powell, R., 1998, An internally consistent thermodynamic data set for phases of petrological interest: *Journal of Metamorphic Geology*, v. 16, p. 309–343. doi:10.1111/j.1525-1314.1998.00140.x
- Keppie, J.D., and Morán-Zenteno, D.J., 2005, Tectonic implications of alternative Cenozoic reconstructions for southern Mexico and the Chortis Block: *International Geology Review*, v. 47, p. 473–491. doi:10.2747/0020-6814.47.5.473
- Krebs, M., Maresch, W.V., Schertl, H.-P., Münker, C., Baumann, A., Draper, G., Idleman, B., and Trapp, E., 2008, The dynamics of intra-oceanic subduction zones: A direct comparison between fossil petrological evidence (Rio San Juan Complex, Dominican Republic) and numerical simulation: *Lithos*, v. 103, p. 106–137. doi:10.1016/j.lithos.2007.09.003
- Krogh Ravn, E.J., and Terry, M.P., 2004, Geothermobarometry of UHP and HP eclogites and schists - an evaluation of equilibria among garnet-clinopyroxene-kyanite-phengite-coesite/quartz: *Journal of Metamorphic Geology*, v. 22, p. 579–592. doi:10.1111/jmg.2004.22.issue-6
- Leake, B.E., Woolley, A.R., Arps, C.E.S., Birch, W.D., Gilbert, M.C., Grice, J.D., Hawthorne, F.C., Kato, A., Kisch, H.J., Krivovichev, V.G., Linthout, K., Laird, J., Mandarino, J., Maresch, W.V., et al., 1997, Nomenclature of amphiboles; report of the subcommittee on amphiboles of the international mineralogical association commission on new minerals and mineral names: *Mineral Mag*, v. 61, p. 295–321. doi:10.1180/minmag.1997.061.405.13
- Leake, B.E., Woolley, A.R., Birch, W.D., Burke, E.A.J., Ferraris, G., Grice, J.D., Hawthorne, F.C., Kisch, H.J., Krivovichev, V.G., Schumacher, J.C., Stephenson, N.C.N., and Whittaker, E.J. W., 2004, Nomenclature of amphiboles: Additions and revisions to the international mineralogical association's amphibole nomenclature: *European Journal of Mineralogy*, v. 16, p. 190–195. doi:10.1127/0935-1221/2004/0016-0191
- Lindsley, D.H., 1983, Pyroxene thermometry: *American Mineralogist*, v. 68, p. 477–493.
- Martens, U., 2009, Geologic evolution of the Maya Block (southern edge of the North American plate): An example of terrane transferal and crustal recycling [Ph.D.]: Stanford University, 166 p. <https://searchworks.stanford.edu/view/7947223>
- Martens, U., Ortega-Obregón, C., Estrada, J., and Valle, M., 2007, Metamorphism and metamorphic rocks, in Bunschuh, J., and Alvarado, G., eds., Central America. Geology, resources and hazards, Volume 1: Taylor & Francis, 485–522 p. <http://www.crcnetbase.com/doi/abs/10.1201/9780203947043.ch19>.
- Martens, U.C., Brueckner, H.K., Mattinson, C.G., Liou, J.G., and Wooden, J.L., 2012, Timing of eclogite-facies metamorphism of the Chuacús complex, Central Guatemala: Record of Late Cretaceous continental subduction of North America's sialic basement: *Lithos*, v. 146–147, p. 1–10. doi:10.1016/j.lithos.2012.04.021
- Martini, M., Mori, L., Solari, L.A., and Centeno-García, E., 2011, Sandstone provenance of the Arperos basin (Sierra de Guanajuato, Central Mexico): Late Jurassic–Early Cretaceous Back-Arc spreading as the foundation of the Guerrero Terrane: *The Journal of Geology*, v. 119, p. 597–617. doi:10.1086/661989
- Martini, M., Solari, L., and Lopez-Martinez, M., 2014, Correlating the Arperos basin from Guanajuato, central Mexico, to Santo Tomas, southern Mexico: Implications for the paleogeography and origin of the Guerrero terrane: *Geosphere*, v. 10, p. 1385–1401. doi:10.1130/GES01055.1
- Morimoto, N., 1988, Nomenclature of pyroxenes: *Mineralogy and Petrology*, v. 39, p. 55–76. doi:10.1007/BF01226262
- Mortensen, J.K., Hall, B.V., Bissig, T., Friedman, R.M., Danielson, T., Oliver, J., Rhys, D.A., Ross, K.V., and Gabites, J.E., 2008, Age and paleotectonic setting of volcanogenic massive sulfide deposits in the Guerrero Terrane of Central Mexico: Constraints from U-Pb age and Pb isotope studies: *Economic Geology*, v. 103, p. 117–140. doi:10.2113/gsecongeo.103.1.117
- Ortega-Gutiérrez, F., Solari, L.A., Ortega-Obregón, C., Elías-Herrera, M., Martens, U., Morán-Ical, S., Chiquín, M., Keppie, J.D., Torres De León, R., and Schaaf, P., 2007, The Maya-Chortís boundary: A tectonostratigraphic approach: *International Geology Review*, v. 49, p. 996–1024. doi:10.2747/0020-6814.49.11.996
- Ortega-Gutiérrez, F., Solari, L.A., Solé, J., Martens, U., Gómez-Tuena, A., Morán-Ical, S., and Reyes-Salas, M., 2004, Polyphase, high-temperature eclogite-facies metamorphism in the Chuacús Complex, central Guatemala: Petrology, geochronology, and tectonic implications: *International Geology Review*, v. 46, p. 445–470. doi:10.2747/0020-6814.46.5.445
- Ortega-Obregón, C., 2005, Caracterización estructural, petrológica y geoquímica de la zona de cizalla "Baja Verapaz", Guatemala [MSc]: Mexico City, Instituto de Geología, Universidad Nacional Autónoma de México, 99 p.
- Ortega-Obregón, C., Solari, L.A., Keppie, J.D., Ortega-Gutiérrez, F., Solé, J., and Morán-Ical, S., 2008, Middle-Late Ordovician magmatism and Late Cretaceous collision in the southern Maya Block, Rabinal-Salamá area, central Guatemala: implications for North America–Caribbean plate tectonics:

- Geological Society of America Bulletin, v. 120, p. 556–570. doi:10.1130/B26238.1
- Pindell, J., Maresch, W.V., Martens, U., and Stanek, K., 2011, The Greater Antillean Arc: Early Cretaceous origin and proposed relationship to Central American subduction mélanges: Implications for models of Caribbean evolution: International Geology Review, v. 54, p. 131–143. doi:10.1080/00206814.2010.510008
- Pindell, J.L., and Barrett, S.F., 1990, Geological evolution of the Caribbean region; A plate-tectonic perspective, in Dengo, G., and Case, J.E., eds., The Caribbean region: Boulder, Colorado, Geological Society of America, The geology of North America, v. H, p. 405–432.
- Pindell, J.L., Cande, S., Pitman, W.C., III, Rowley, D.B., Dewey, J.F., Labrecque, J., and Haxby, W., 1988, A plate-kinematic framework for models of Caribbean evolution: Tectonophysics, v. 155, p. 121–138. doi:10.1016/0040-1951(88)90262-4
- Pindell, J.L., and Kennan, L., 2009, Tectonic evolution of the Gulf of Mexico, Caribbean and northern South America in the mantle reference frame: An update: Geological Society, London, Special Publications, v. 328, p. 1–55. doi:10.1144/SP328.1
- Plafker, G., 1976, Tectonic aspects of the Guatemala earthquake of 4 February 1976: Science, v. 193, p. 1201–1208. doi:10.1126/science.193.4259.1201
- Proyer, A., McCammon, C., and Dachs, E., 2004, Pitfalls in geothermobarometry of eclogites: Fe<sup>3+</sup> and changes in the mineral chemistry of omphacite at ultrahigh pressures: Contributions to Mineralogy and Petrology, v. 147, p. 305–318. doi:10.1007/s00410-004-0554-6
- Ratschbacher, L., Franz, L., Min, M., Bachmann, R., Martens, U., Stanek, K., Stübner, K., Nelson, B.K., Herrmann, U.R., Weber, B., López-Martínez, M., Jonckheere, R., Sperner, B., Tichomirowa, M., et al., 2009, The north American-Caribbean Plate boundary in Mexico-Guatemala-Honduras: Geological society: London, Special Publications, v. 328, p. 219–293. doi:10.1144/SP328.11
- Ravna, K., 2000, The garnet-clinopyroxene Fe<sup>2+</sup>-Mg geothermometer: An updated calibration: Journal of Metamorphic Geology, v. 18, p. 211–219. doi:10.1046/j.1525-1314.2000.00247.x
- Rogers, R.D., Mann, P., Emmet, P.A., and Venable, M.E., 2007, Colon fold belt of Honduras: Evidence for Late Cretaceous collision between the continental Chortis block and intra-oceanic Caribbean arc, in special paper 428: Geologic and tectonic development of the Caribbean plate boundary in northern Central America: Geological Society of America, v. 428, p. 129–149.
- Rojas-Agramonte, Y., Kröner, A., García-Casco, A., Somin, M., Iturralde-Vinent, M., Mattinson, J. M., Millán Trujillo, G., Sukar, K., Pérez Rodríguez, M., Carrasquilla, S., Wingate, M. T. D. and Liu, D. Y., 2011, Timing and Evolution of Cretaceous Island Arc Magmatism in Central Cuba: Implications for the History of Arc Systems in the Northwestern Caribbean: The Journal of Geology, v. 119, p. 619–640.
- Schwartz, D.P., Cluff, L.S., and Donnelly, T.W., 1979, Quaternary faulting along the Caribbean-North American plate boundary in Central America: Tectonophysics, v. 52, p. 431–445. doi:10.1016/0040-1951(79)90258-0
- Siivola, J., and Schmidt, R., 2007, List of mineral abbreviations, in Fettes, D.J., Desmons, J., and Arkai, P., International Union of Geological Sciences, eds., Metamorphic rocks: A classification and glossary of terms: recommendations of the International Union of geological sciences, Subcommittee on the systematics of metamorphic rocks, Cambridge; New York, Cambridge University Press, 93–109 p.
- Solari, L.A., García-Casco, A., Martens, U., Lee, J.K.W., and Ortega-Rivera, A., 2013, Late cretaceous subduction of the continental basement of the Maya Block (Rabinal Granite, central Guatemala): Tectonic implications for the geodynamic evolution of Central America: Geological Society of America Bulletin, v. 125, p. 625–639. doi:10.1130/B30743.1
- Solari, L.A., Gómez-Tuena, A., Ortega-Gutiérrez, F., and Ortega-Obregón, C., 2011, The Chuacús Metamorphic Complex, central Guatemala: Geochronological and geochemical constraints on its Paleozoic - Mesozoic evolution: Geologica Acta, v. 9, p. 329–350.
- Stanek, K.P., Maresch, W.V., and Pindell, J.L., 2009, The geotectonic story of the northwestern branch of the Caribbean Arc: Implications from structural and geochronological data of Cuba: Geological Society, London, Special Publications, v. 328, p. 361–398. doi:10.1144/SP328.15
- Sutter, J., 1979, Late Cretaceous collisional tectonics along the Motagua fault zone, Guatemala: GSA Abstracts with Programs, v. 11, p. 525–526.
- Tsujimori, T., and Harlow, G.E., 2012, Petrogenetic relationships between jadeitite and associated high-pressure and low-temperature metamorphic rocks in worldwide jadeitite localities: A review: European Journal of Mineralogy, v. 24, p. 371–390. doi:10.1127/0935-1221/2012/0024-2193
- Tsujimori, T., Liou, J.G., and Coleman, R.G., 2004, Comparison of two contrasting eclogites from the Motagua Fault Zone, Guatemala: Southern lawsonite eclogite versus northern zoisite eclogite, in Denver: Geologic Society of America. [http://gsa.confex.com/gsa/2004AM/finalprogram/abstract\\_79984.htm](http://gsa.confex.com/gsa/2004AM/finalprogram/abstract_79984.htm). (accessed December 2011).
- Tsujimori, T., Liou, J.G., and Coleman, R.G., 2005, Coexisting chromian omphacite and diopside in tremolite schist from the Chugoku Mountains, SW Japan: The effect of Cr on the omphacite-diopside immiscibility gap: American Mineralogist, v. 89, p. 7–14. doi:10.2138/am-2004-0102
- Tsujimori, T., Sisson, V.B., Liou, J.G., Harlow, G.E., and Sorensen, S.S., 2006a, Petrologic characterization of Guatemalan lawsonite eclogite: Eclogitization of subducted oceanic crust in a cold subduction zone, in Hacker, B.R., McClelland, W.C., and Liou, J.G., eds., Ultrahigh-pressure metamorphism: Deep continental subduction, Volume 403: Geologic Society of America, GSA Special Papers, 147–168 p.
- Tsujimori, T., Sisson, V.B., Liou, J.G., Harlow, G.E., and Sorensen, S.S., 2006b, Very-low-temperature record in subduction process. A review of worldwide lawsonite eclogites: Lithos, v. 92, p. 609–624. doi:10.1016/j.lithos.2006.03.054
- van den Boom, G., 1972, Petrofazielle Gliederung des metamorphen Grundgebirges in der Sierra de Chuacús, Guatemala.: Bundesanstalt für Bodenforschung, Geologisches Jahrbuch: Beiheft, v. 122, p. 49.
- van den Boom, G., Müller, A., Nicolaus, H.-J., Paulsen, S., and Reyes, J., 1971, Geologische Übersichtskarte Baja Verapaz und Südteil der Alta Verapaz, 1:125,000, Hannover, Bundesanstalt für Bodenforschung.
- Yui, T.-F., Maki, K., Usuki, T., Lan, C.-Y., Martens, U., Wu, C.-M., Wu, T.-W., and Liou, J.G., 2010, Genesis of Guatemala jadeitite and related fluid characteristics: Insight from zircon: Chemical Geology, v. 270, p. 45–55. doi:10.1016/j.chemgeo.2009.11.004